Oyster aquaculture impacts on benthic nitrogen cycling and efficacy as a nutrient bioextraction tool in a tributary of Chesapeake Bay

Abby M. Lunstrum
Camas, WA

BS, Ecology/Evolution/Conservation Biology, University of Washington, 2006

A Thesis presented to the Graduate Faculty of the University of Virginia
in Candidacy for the Degree of Master of Science

Department of Environmental Sciences
University of Virginia
December, 2015

Abstract

Oysters are popularly thought to improve water quality by filtering plankton and associated nutrients from the water column, and oyster aquaculture and reef restoration have thus been proposed as tools to reduce nutrient pollution in coastal areas. However, oysters' net effect on water quality, including indirect impacts associated with altered sediment nutrient cycling, remains poorly understood. This study assessed the impacts of oyster aquaculture on sediment nitrogen (N) processes—including denitrification, dissimilatory nitrate reduction to ammonium (DNRA), and fluxes of dissolved nutrients—at a commercial oyster farm in Cherrystone Inlet, VA, a tributary of Chesapeake Bay. Denitrification was significantly enhanced in farm sediments, but rates were low (< 20 μm N m^{-2} h^{-1}) and appeared to be limited by sediment anoxia and inhibited nitrification. Furthermore, DNRA was the dominant nitrate reduction pathway, accounting for an average of 70% of nitrate reduction. Ammonium flux to the water column was the most significant measured pathway in the farm, exceeding 900 μm N m^{-2} h^{-1} in summer. Extrapolating the observed annual rates to the area leased for aquaculture in the inlet, N extractive processes—including harvest, enhanced denitrification, and enhanced accumulation in sediment—could remove 160% of the annual N load. However, the enhanced ammonium flux from sediment to the water column was comparable in magnitude to total N extraction, potentially supporting local N recycling and eutrophication. Negative impacts associated with eutrophication were not currently apparent in the inlet, likely due to active farm management and high tidal flushing. Thus, oyster aquaculture may be an effective tool to reduce nutrient concentrations in this location and similar water bodies with moderate N loads, high tidal flushing, and significant area for aquaculture expansion.

Acknowledgements

I am grateful to my committee members—Karen McGlathery, Mike Pace, Aaron Mills, and Jim Galloway—for their helpful advice and support throughout my research. I extend special thanks to my advisor, Karen McGlathery, for accepting an unsolicited student application from China, for having faith in my research direction, and for providing space and support for my professional growth. I am also especially grateful to Mike Pace for his advice and encouragement on experimental and technical issues, especially regarding the membrane inlet mass spectrometer. The appendix to Chapter 1 would not exist without his support.

I am indebted to many colleagues for their advice, support, and cooperation during this research. In particular, I am grateful to my labmate Lillian Aoki for her consistent helpfulness and inspiration. Matthew Oreska and Marie Lise Delgard similarly provided valuable field and lab assistance and feedback on my research that I am extremely grateful for. I also received help and advice from former labmates Kyle Emery and Alia Al-Haj. Ashley Smyth at VIMS was a constant source of support and encouragement for benthic flux measurements. Suzanne Bricker, at NOAA, was an invaluable help and role model over the past two years. Todd Kana provided exceptional feedback and technical support for the MIMS. Finally, I am very grateful for the help of several undergraduate field and laboratory assistants, including: Amy Bartenfelder, Kendall Combs, Bridget Shayka, and in particular Meigan McManus and Devin Rowell who contributed to my work over several semesters.

I would like to extend special thanks to the staff at Virginia Sea Grant for funding my research, for their enthusiastic support, and for providing opportunities to extend the impact of my work.

Finally, I would like to thank Chris and Jennifer Buck at Ruby Salts Oyster Farm for their enthusiasm and support of my research. This research would not have been possible without their cooperation.

Table of contents

List of figures

List of tables

Introduction

Bivalve aquaculture has expanded significantly over the past several decades and now accounts for over 70% of global marine aquaculture production (Campbell and Pauly, 2013). Oysters alone constitute one third of this sector (FAO, 2011). Oysters are popularly thought to have positive impacts on coastal water quality, as they filter plankton from the water column, effectively removing reactive nitrogen (N) and reducing the effects of eutrophication. Because of this, harvest of aquacultured oysters has been proposed as a tool to mitigate coastal eutrophication through "nutrient bioextraction". However, oysters can also impact water quality indirectly by altering sediment N cycling, and these processes remain poorly studied. Assessing the balance between benthic processes that remove reactive N from, or return reactive N to the water column is important for understanding oyster aquaculture's net impact on coastal water quality.

This thesis explores a) how oyster aquaculture impacts benthic N cycling and b) its potential effectiveness as a nutrient bioextraction tool. Both research objectives were conducted at a commercial *Crassostrea virginica* oyster farm in a tributary of Chesapeake Bay.

Chapter 1 focuses on benthic N cycling and fluxes in the farm and at a reference site. Denitrification, dissimilatory nitrate reduction to ammonium (DNRA), and associated fluxes, including dissolved inorganic N (DIN) and oxygen (O_2) were measured six times in 2013-2014 using sediment core incubations and the Isotope Pairing Technique (IPT). Denitrification was enhanced within the farm by an annual average of 300%, but absolute rates remained low, reaching a maximum of 19.2 μmol N m^{-2} h^{-1}. Denitrification appeared to be inhibited by low nitrification, resulting from sediment anoxia. Direct ammonium flux to the water column was the dominant N pathway in the farm, which lowered denitrification efficiency relative to the reference site. DNRA was consistently more important than denitrification, and accounted for an average of 70% of nitrate (NO_3^-) reduction at all sites. These results suggest that although denitrification was enhanced within the oyster farm, N cycling was shifted toward

regeneration of reactive N to the water column. Thus, considering enhanced denitrification as a nutrient extraction pathway may be misleading.

During analysis for Chapter 1, my colleague Lillian Aoki and I discovered a previously undocumented issue affecting denitrification measurements with IPT using the membrane inlet mass spectrometer (MIMS). This issue is described in the Appendix to Chapter 1. Oxygen interference on the MIMS significantly altered N_2 isotope values, potentially causing artificially high estimates of denitrification rates. Both laboratory tests and comparative analysis of sediment incubations performed for Chapter 1 showed that O_2 interference could inflate denitrification by >100 μmol N m^{-2} h^{-1} above actual rates. Based on these results, we recommend that future studies utilizing MIMS and IPT remove O_2 from samples with a furnace and reduction column inline with the MIMS.

Chapter 2 combines the denitrification rates from Chapter 1 with harvest and burial rates to assess the total N bioextraction potential of the farm. Chapter 2 also includes discussion of the balance between total N extraction and benthic N regeneration, and how these rates compare to watershed N loading. Of the three extractive pathways, harvest was the most significant, accounting for 69% of total removal. Enhanced burial contributed an additional 30% and enhanced denitrification was insignificant at <1%. When extrapolated to the total area leased for aquaculture in Cherrystone Inlet, bioextraction could remove 162% of the estimated N load. Regeneration of reactive N from the sediment was similar in magnitude to total N bioextraction, posing a potential eutrophication concern. However, ambient N concentrations were low, and farm maintenance and high tidal flushing are believed to export enhanced primary productivity from the inlet. Thus, in this location, it appears that N extraction can significantly mitigate watershed N loads without adverse consequences of eutrophication.

These chapters cumulatively explore how oyster aquaculture impacts coastal water quality directly via N assimilation and indirectly by altering sediment N processes. As oyster aquaculture expands, and debate about its use as nutrient bioextraction tool continues, understanding these

pathways is critical to sustainable growth of the industry. The field measurements and analysis in this study provide valuable and pertinent information to inform decisions balancing oyster aquaculture and coastal water quality objectives.

References

Campbell, B., Pauly, D., 2013. Mariculture: A global analysis of production trends since 1950. Marine Policy 39, 94–100.

FAO, 2011. FAO Fisheries and Aquaculture Department. World aquaculture 2010. Technical Paper. No. 500/1. Rome.

Chapter 1.

Enhanced but limited denitrification at a *Crassostrea virginica* oyster aquaculture farm in a tributary of Chesapeake Bay*

*To be submitted for publication with the following intended co-authors: Karen McGlathery, Ashley Smyth

Abstract

Filter-feeding bivalves like oysters couple pelagic primary production with benthic microbial processes by consuming plankton from the water column and depositing unassimilated material on the sediment surface. Conceptual models suggest that at low to moderate oyster density, this deposition can stimulate the loss of reactive nitrogen (N) by providing sediment denitrifying bacteria with organic carbon and N. While enhanced sediment denitrification has been found at oyster reefs, the limited data available for oyster aquaculture have not found the predicted enhancement. This study quantified seasonal rates of denitrification, as well as dissimilatory nitrate reduction to ammonia (DNRA), and dissolved inorganic N fluxes at a rack and bag eastern oyster (*Crassostrea virginica)* aquaculture farm. Consistent with the conceptual model, denitrification was enhanced within the farm compared to the adjacent reference site, with an average annual increase of 300%. However, absolute denitrification rates were low relative to rates from other coastal studies, reaching a maximum of 19.2 μmol m^{-2} h^{-1} underneath oyster culture. Denitrification was limited in the farm by low NO_3^- availability, resulting from low nitrification in anoxic sediments, which was likely caused by high rates of biodeposition. Consequently, direct release of ammonium (NH_4^+) to the water column was the most significant benthic N pathway, with rates over 900 μmol m^{-2} h^{-1} underneath oyster racks in summer. Denitrification may also have been limited by DNRA, which accounted for an average of 70% of NO_3^- reduction at all sites. The enhanced N processes in the farm were spatially limited, with significantly higher rates directly under, compared to in between oyster racks. For oyster densities typical of commercial aquaculture farms, denitrification may be enhanced, but nonetheless limited by biodeposition-induced sediment anoxia and DNRA dominance. The resulting shift in the sediment N balance toward processes that regenerate reactive N to the water column is an important consideration for water quality.

Introduction

Bivalves alter coastal ecosystem dynamics by filtering plankton from the water column and concentrating organic matter (OM) in tissue and on nearby sediment. This filtering can have a direct positive impact on water quality by reducing turbidity and facilitating the growth of submerged aquatic vegetation (Newell 2004). However, bivalves can also impact water quality indirectly, as OM deposited on the sediment surface can alter sediment nitrogen (N) cycling. For example, particulate N can be remineralized and released to the water column as ammonium (NH_4^+), a form of biologically reactive N (Dame et al. 1992; Bartoli et al. 2001). High concentrations of reactive N can subsequently lead to eutrophication and related adverse ecological impacts (Nixon 1995). Conversely, some of the N may be converted by denitrification to nitrogen gas (N_2), a non-reactive form of N which will exit the aquatic system (Newell et al. 2002). The balance between denitrification and processes that return reactive N to the water column helps determine whether oysters may improve water quality or potentially contribute to eutrophication. Thus, understanding this balance is important for assessing the net impact of bivalves on coastal water quality.

Oyster biodeposits can potentially enhance denitrification by increasing delivery of organic C and N to the sediment (Newell 2004). Denitrifying bacteria utilize organic C to reduce NO_3^- and other nitrogen oxides (henceforth referred to collectively as NO_3^-) to N_2. Nitrate can either be supplied from the water column in high NO_3^- environments, or from NO_3^- produced in the sediment by nitrification of NH_4^+. The latter process, commonly referred to as coupled nitrification-denitrification, may also be enhanced by the organic subsidy from biodeposition, as organic N is mineralized and subsequently nitrified. However, nitrification is an obligate aerobic process, so coupled nitrification-denitrification also depends on sufficient sediment O_2 levels (Jenkins and Kemp 1984). Thus, biodeposition alone may not stimulate denitrification in all situations, as O_2 concentration and/or NO_3^- availability are also important.

Cultivation method and oyster density may affect denitrification rates in oyster aquaculture by altering the availability of these components. Conceptual models and lab-based results using algal pellets as biodeposit proxies suggest that at low to moderate oyster densities, biodeposition stimulates denitrification, but at higher densities, excessive OM loading can deplete sediment O_2 and thus inhibit coupled nitrification-denitrification (Figure 1) (Newell et al. 2002; Newell 2004). Some field studies at mussel farms and oyster reefs have found this pattern, with enhanced denitrification at moderate densities and relatively lower denitrification at very high densities (Carlsson et al. 2012; Smyth et al. 2015). For example, Smyth et al. (2015) found denitrification in oyster reef sediment increased with density up to a threshold of 2,400 oysters m^{-2}, beyond which denitrification decreased. This density is much higher than typical oyster farms, which average 100-200 oysters m^{-2}. Oyster cultivation method may similarly affect denitrification rates by concentrating or diluting biodeposits, thus affecting both the delivery of organic C and potential for sediment O_2 depletion. Oysters may be cultivated in relatively deep water in floating cages or suspended lines; directly on the sediment surface; or slightly above the sediment using near bottom methods like cages or racks and bags. In floating or suspended applications, biodeposits may be distributed over larger areas, potentially diluting effects on benthic processes. To date, denitrification has only been measured in floating-type oyster aquaculture settings, and the limited data have not shown significant enhancement of denitrification (Holyoke 2008; Higgins et al. 2013). No study has yet measured denitrification in a near-bottom oyster aquaculture setting.

Another consideration that can potentially impact denitrification rates is the prevalence of dissimilatory nitrate reduction to ammonium (DNRA). DNRA is an alternative, microbial NO_3^- reduction pathway that competes with denitrification by utilizing the same electron acceptor (NO_3^-). Unlike denitrification, DNRA results in the retention of reactive N (in the form of NH_4^+) within the system, and thus can maintain or contribute to, rather than reduce eutrophic conditions. Measurements of DNRA in oyster aquaculture are even more limited than for denitrification. Potential rates indicate that DNRA

may be significant in oyster farms (Gilbert et al. 1997), and in studies of other farmed bivalve species, DNRA often dominates NO_3^- reduction (Christensen et al. 2000; Nizzoli et al. 2006). However, oyster reefs have shown low DNRA potential relative to denitrification (Smyth et al. 2013). Thus, it is still unclear if DNRA is an important consideration in oyster aquaculture N cycling.

DNRA and mineralization of deposited particulate N can both contribute to benthic NH_4^+ flux from sediments to the overlying water. Because the balance between NH_4^+ flux and denitrification contributes to the net impact of oyster aquaculture on coastal water quality, it is important to consider these N processes simultaneously. For example, even if denitrification is enhanced in oyster farms, if NH_4^+ efflux is enhanced to a greater degree, eutrophic conditions could be supported relatively more than in unimpacted areas. Benthic NH_4^+ regeneration to the water column is well documented in oyster aquaculture systems, with most studies showing enhanced fluxes (Mazouni et al. 1996; Chapelle et al. 2000; Higgins et al. 2013). In cases with very high rates of biodeposition, sediment anoxia and inhibited nitrification can further shift benthic N cycling toward mineralization and enhanced benthic NH_4^+ flux (Carlsson et al. 2012). Sediment anoxia also leads to the accumulation of alternative reduced species like iron(II) and sulfides, which shift N processes toward N mineralization, DNRA (Christensen et al. 2000), and the release of soluble reactive phosphorus (SRP), which can also contribute to eutrophication (Correll 1998). In some situations, enhanced NH_4^+ fluxes associated with oyster farms may result in additional ecological impacts. For example, high concentrations of NH_4^+ near bivalve farms may stimulate harmful algal blooms (HABs), which are increasing in occurrence (Heisler et al. 2008; Bouwman et al. 2011).

There is currently interest in using bivalve aquaculture to extract N from eutrophic coastal waters, as some of the consumed N is incorporated into tissue and can be harvested, and also on the assumption that sediment denitrification may be enhanced (Carmichael et al. 2012; J Rose et al. 2014). Using oysters for this purpose is commonly referred to as “nutrient bioextraction.” Despite bivalve

aquaculture's potential to remove N directly via harvest, the potential impacts of on sediment N cycling, especially high NH_4^+ flux, and the poorly defined balance between denitrification and N regeneration, has fueled significant debate (Stadmark and Conley 2011; Petersen et al. 2012; JM Rose et al. 2012; Stadmark and Conley 2012). As a result, oyster aquaculture has yet to be widely accepted as a nutrient bioextraction tool.

To inform this debate, we quantified benthic denitrification, DNRA, and nutrient fluxes at a near-bottom oyster farm, with oyster densities typical of commercial farms. We specifically aimed to test the hypothesis that denitrification was enhanced within the farm relative to an uncultivated site, as a result of biodeposition from "moderate" oyster densities. To complement the denitrification data, we also measured benthic processes that contribute to N regeneration including DNRA and total NH_4^+ flux, as well as related fluxes of oxygen (O_2) and soluble reactive phosphorus (SRP). Finally, we assessed the spatial variability of these rates within the farm by considering locations directly below oysters as well as in between oyster racks (approximately 1 m from oysters).

Methods

Site description

Cherrystone Inlet is a shallow tributary of the lower Chesapeake Bay on the Virginia Eastern Shore, USA (Figure 2). Situated approximately 25 km from the mouth of the Bay, Cherrystone is characterized by relatively high tidal flushing, with a tidal prism of approximately 1/2 the inlet volume per day, and salinity fluctuates between 17 and 27 parts per thousand (ppt) (Kuschner 2015). The inlet covers 5.7 km^2, with a mean depth of 1.1 m at mean sea level. The extensive shallow areas along the inlet's perimeter support large areas of bivalve aquaculture, primary hard clam (*Mercenaria mercenaria*), with smaller areas of eastern oyster (*Crassostrea virginica*) cultivation. The farm in this study cultivates eastern oysters using the "French" rack and bag method, in which oysters are grown in mesh bags

(approximately 50 x 90 cm), on racks approximately 30 cm above the sediment surface. Oyster density ranged from 300 individual oysters per bag for harvest class to 1200 individuals per bag for seed < 2.5 cm in diameter. At the time of this study, the farm had been in operation for four years and occupied approximately 1000 m^2. Annual seeding added 130,000 oyster seeds, and harvest was approximately 65,000 market-sized oysters. The average areal oyster density—70 harvested oysters m^{-2}, or a seeding density of 140 oyster m^{-2} with an observed 50% mortality rate—is typical of commercial oyster farms (Rose et al., 2015; Don Webster, personal communication). The farm is subtidal, although sediment at the near-shore edge of the farm is exposed during low-low tides.

Environmental characteristics

Triplicate surface sediment samples (0-2 cm) were collected at randomly selected locations for each site, once per season (October, January, April, and June) to assess sediment porosity, dry bulk density, and carbon (C) and N content. Samples were collected with 2.6-cm ID corer, weighed, and dried to constant weight at 60° C. Carbon and N contents (% dry weight) were measured with 25-mg aliquots on a Carlo Erba NA 2500 Elemental Analyzer.

Sediment grain size distribution (0-2 cm depth) was assessed for each site in July 2014. Triplicate samples were collected at randomly selected locations for each site with a 60-ml cut-off syringe and stored at 5° C. Samples were oxidized and acidified to remove OM and carbonates, respectively, prior to analysis. Organic matter was removed by slowly adding approximately 20 ml of H_2O_2 to 10 g (estimated dry weight) subsamples for each site. Potential carbonates were removed by adding 30 ml of sodium acetate solution (pH 5), shaking for 30 minutes, and rinsing with deionized water. One ml of dispersing agent (sodium hexametaphosphate) was added to each sample prior to analysis on a Beckman Coulter Laser Diffraction Particle Size Analyzer (LS 13 320).

Benthic chlorophyll *a* (a proxy for benthic microalgae) was measured in April and June 2015. Surface samples (0-1 cm depth) were collected at six random locations for each site using a 1.3-cm ID corer, and analyzed spectrophotometrically according to the method of Lorenzen (1965), which accounts for possible phaeopigments.

In situ water temperature and salinity were measured during each sample collection with a handheld glass thermometer and refractometer, respectively. Ambient water samples were also collected for dissolved nutrient analysis. Samples were filtered to remove particulate matter (0.45-µm pore size GFF filters) and frozen until analysis by standard colorimetric methods on a flow-injection nutrient autoanalyzer (Lachat). Nitrite plus nitrate concentrations were assessed by reduction of NO_3^- to NO_2^- and analyzed with Lachat QuikChem method 31-107-04-1-E; ammonium concentrations were analyzed by method 31-107-06-1-B; and SRP concentrations with method 31-115-01-1-H. Lower detection limits were 0.36 µM for NH_4^+ and NO_3^-0.16 µM for SRP.

Core incubations

*S*ediment cores were collected six times between July 2014 and June 2015 (July, August, October, January, April, and June). Sediment cores were collected at a reference site 40 m from the farm ("Bare"), and two distinct areas within the farm: directly under oyster bags ("Oyster"), and in between racks ("Row"). Row sites were approximately 1 m from the nearest oyster bag, and subjected to regular disruption during daily to weekly farm maintenance. For each site, triplicate or quadruplicate cores were collected at randomly selected locations, using acrylic cylinders (30-cm depth by 10-cm ID), with approximately 12 cm of sediment and 18 cm of overlying water. Custom core bottoms fitted with o-rings were applied in the field, and cores were loosely capped during transport to the laboratory.

Cores were kept at or below in situ temperatures and returned to the laboratory within four hours, at which point they were submerged in a common bath filled with ~150 l of unfiltered site water.

The bath was maintained at in situ temperature, and cores were pre-incubated overnight with aquarium bubblers to ensure fully oxygenated starting conditions. Water blanks were also incubated concurrently to assess water column activity. At the start of the incubations, all cores were gently cleared of bubbles, and sealed with custom lids. Lids were fitted with magnetic stir bars to ensure a mixed water column throughout the incubation, and inlet and outlet ports for sampling the water column. During sampling, water samples were forced by gravity from a reservoir also maintained at in situ temperature.

Incubations were conducted in the dark for 3 to 8 hours, depending on season, aiming for average O_2 depletion of 30% (i.e., $T_f = 0.7\ T_0$) with no cores falling below 3 mg $O_2\ l^{-1}$. Cores were incubated twice in succession during each experiment, as described in detail below. The first incubation assessed sediment O_2 and benthic fluxes of dissolved inorganic nutrients, including SRP, NH_4^+, and nitrite (NO_2^-) plus NO_3^-. Benthic fluxes of nitrous oxide (N_2O) were also measured during the first incubation in April 2015. The second incubation was conducted with added $^{15}NO_3^-$ to assess denitrification and DNRA with the isotope pairing technique (IPT) (Nielsen 1992).

Incubation #1: Nutrients, O_2, N_2O

Benthic fluxes of nutrients, O_2, and N_2O, were measured by taking water samples from each core immediately after capping (T_0), and at the end of the incubation (T_f). Oxygen was monitored in one representative core intermittently to assure sufficient O_2 levels. Samples for O_2 were collected in 12 ml Exetainer vials (Labco), with the addition of 40 µl of 100% (m/v) $ZnCl_2$ solution, and then stored under water at or below incubation temperature until analysis on a membrane inlet mass spectrometer (MIMS). Dissolved nutrient concentrations were measured for all incubations except July 2014, and processed and analyzed as described above for environmental characteristics. In April 2015, samples for N_2O analysis were collected in 40-ml serum bottles (Wheaton) with the addition of 60 µl $ZnCl_2$ solution, stored at room temperature, and analyzed by headspace gas chromatography (Shimadzu GC-2014). All

analyses with the exception of N_2O were conducted at the University of Virginia; N_2O samples were analyzed at Boston University.

Benthic fluxes for all analytes were calculated per core basal area (i.e., sediment area) as:

$$Flux = \frac{([x]_{Tf} - [x]_{T0}) * V}{A * T} \quad (1)$$

where $[x]_{Tf}$ and $[x]_{T0}$ are analyte concentrations at T_f and T_0, respectively; *V* is water column volume in each core; *A* is sediment surface area; and *T* is the duration of the incubation. Fluxes were corrected for water column activity determined from the water blanks.

Incubation #2: Denitrification and DNRA

Following the first incubation, cores were uncapped and re-oxygenated with aquarium bubblers for two hours. The common bath water was then sampled to measure initial NO_3^- concentration, and a sodium ^{15}N-nitrate solution (minimum 98% ^{15}N, Cambridge Isotopes) was added to yield a final water column concentration of approximately 30 µM NO_3^-. The bath water, including the water overlying each core, was gently mixed for 20 minutes to ensure sufficient mixing of the amended ^{15}N to the sediment surface (Steingruber et al. 2001). The cores were then capped and T_0 samples taken from the water column to start the incubation.

The incubation was run for a similar length of time as the first, after which the bath water was lowered, and the cores uncapped. Upon uncapping, a subsample of the core (sediment and water column) was extracted for DNRA analysis using methods adapted from Nizzoli et al. (2006). In brief, subsamples were extracted with a 2.2 cm ID acrylic pipe, mixed with powdered KCl (sufficient to 2N solution) to extract NH_4^+, and then frozen for later analysis (described below). The remaining core was then gently mixed with a rod until homogenous, allowed to settle for 60 seconds, and a slurry sample collected for T_f. Samples were slurried to ensure capture of $^{29}N_2$ and $^{30}N_2$ produced during the incubation, which can be elevated in pore water over short incubation times (as summarized in

Steingruber et al., 2001). Samples were collected in 12 ml vials (Exetainer), treated with 60 µl 100% $ZnCl_2$ solution, and stored under water at or below incubation temperature until analysis.

IPT and DNRA analysis

IPT samples were analyzed for $^{29}N_2$ and $^{30}N_2$ on the MIMS with an in-line furnace and copper reduction column heated to 600° C to remove O_2. Variable O_2 concentrations between samples can influence the mass to charge ratio (m/z) signals 29 and 30 (corresponding primarily to $^{29}N_2$ and $^{30}N_2$) and lead to artificially enhanced denitrification rates (Lunstrum and Aoki 2015). The magnitude of this effect is believed to be machine-specific and may be minor with small changes in O_2 concentration. However, our MIMS exhibited significant impacts on m/z 29 and 30 signals with O_2 depletion beyond 50%. In this study, although water column O_2 at T_f was on average 70% of T_0, slurry O_2 concentrations dropped to <1% of T_0 values in some cores, likely a result of rapid geochemical oxidation of highly reduced sediment. Thus, a furnace was necessary for accurate calculation of denitrification rates.

Areal production rates of $^{29}N_2$ and $^{30}N_2$ ($p^{29}N_2$ and $p^{30}N_2$, respectively) were calculated with Eqn. 1, using total water volume, including water column and pore water, for T_f. Denitrification of added $^{15}NO_3^-$ (D15) and in situ NO_3^- (D14) were then calculated using standard IPT equations (Nielsen 1992). D15 is an indication of denitrification potential, while D14 is the estimated in situ denitrification rate. IPT equations require that anammox is not a significant source of N_2. We assumed insignificant anammox contribution in our cores, since anammox is consistently low in shallow (<10 m) coastal areas (Thamdrup and Dalsgaard 2002) and often in low NO_3^- environments (Risgaard-Petersen et al. 2004). Anammox has specifically been found to occur at relatively insignificant rates (<10% of N_2 production) in oyster aquaculture sediment (Higgins et al. 2013).

Considering both NH_4^+ flux and denitrification, we also calculated the denitrification efficiency (DE) for each site. DE was calculated for each core as the ratio of denitrification to the sum of positive fluxes of denitrification, NH_4^+, and NO_3^-.

DNRA was quantified with a modification of the OX/MIMS technique, which utilizes MIMS to measure N_2 produced by oxidation of NH_4^+ (Yin et al. 2014). Thawed KCl slurry samples were mixed for 30 minutes on a shaker table, filtered to remove particulate matter (0.45 μm pore size), and then transferred to duplicate 12-ml vials (Exetainer). One of each sample pair was injected with 0.2 ml of alkaline hypobromite iodine solution to oxidize $^{15}NH_4^+$ to $^{30}N_2$ or $^{29}N_2$ (a product of $^{15}NH_4^+$ combination with $^{14}NH_4^+$). $^{29}N_2$ and $^{30}N_2$ were then measured on the MIMS with in-line furnace. Background $^{29}N_2$ and $^{30}N_2$ values determined for the un-oxidized sample (primarily products of denitrification during the incubation) were subtracted from the oxidized sample to quantify the $^{29}N_2$ and $^{30}N_2$ produced by the hypobromite oxidation of $^{15}NH_4^+$. Production rates of $^{29}N_2$ and $^{30}N_2$ were then calculated per Eqn 1. DNRA stimulated by the $^{15}NO_3^-$ addition ($DNRA_{15}$) was subsequently calculated as the sum of $^{29}N_2$ and $^{30}N_2$ production, per:

$$DNRA_{15} = p(^{29}N_2) + 2p(^{30}N_2) \quad (2)$$

In situ DNRA ($DNRA_{14}$) was calculated based on the assumption that the relative rates of DNRA utilizing $^{15}NO_3^-$ and $^{14}NO_3^-$ occur at the same ratio as that for denitrification (Risgaard-Petersen and Rysgaard 1995):

$$DNRA_{14} = DNRA_{15} \times \frac{D14}{D15} \quad (3)$$

Statistical analysis

Statistical differences for benthic fluxes, denitrification, DNRA, and derived factors (e.g., denitrification efficiency) were assessed by two-way analysis of variance (ANOVA) with site type and sampling date as fixed factors. Differences between sediment characteristics at each site were assessed

with one-way ANOVA. Normality and homogeneity of variance were both assumed, as sample sizes were equal or similar (n= 3 to 4) and consequently the difference between nominal and actual significance values conservative and/or small (Glass et al. 1972). Post-hoc Tukey HSD tests were used to assess significant differences between sites. All analyses were done with SPSS v 22, with a significance level of α=0.05.

Results

Environmental characteristics

Water temperature ranged from near freezing in January when ice was present on the water surface, to 30° C in July (Table 1). Salinity was relatively consistent, ranging between 23 and 27 ppt. Dissolved inorganic nutrient concentrations (NH_4^+, NO_3^-, and SRP) also varied little, and were very low and near or below detectable limits in all seasons. NH_4^+ was slightly elevated (<2 µM) however, during the July and April samplings.

Sediment properties were visibly different between sites, with Oyster sediment finer and more porous than Row and Bare. Porosity was on average 20% higher, and statistically different, at Oyster compared to Bare and Row sites (p<0.0005) (Table 2). Conversely, sediment dry bulk density at Oyster sites was substantially lower than at the other two sites (p<0.0005). For both parameters, Row sites were more similar to Bare than nearby Oyster sites. C and N concentrations were low at all sites, but enriched within the farm relative to Bare sites. Bare sites averaged 0.16% C and 0.04% N, while Row and Oyster sediments had 0.36% and 1.00% C respectively, and 0.06% and 0.14% N respectively. For both parameters, Oyster sediments were statistically different from Bare and Row sites (p<0.003 for C and p<0.019 for N). Sediment grain size was significantly lower within the farm, with 19.8 to 22.8% silt and clay composition at farm sites compared to 5.6% at the Bare sites (p<0.003).

Benthic chlorophyll *a* was higher within the farm in April, when concentrations at the Oyster site were 37.9 (±1.9 standard error) mg m^{-2}, nearly double Bare and Row (22.0 ± 4.5 and 15.2 ± 3.0 mg m^{-2}, respectively). However, in June, all three sites had similar concentrations (32.1 to 37.6 mg m^{-2}), and overall the sites were not significantly different (p=0.81).

Sediment O_2, Nutrient, and N_2O Fluxes

Oxygen fluxes varied seasonally, with the highest sediment O_2 demand (i.e., O_2 flux into sediment, indicated by negative values) in spring, followed by summer (Figure 3). Oyster sites had the highest sediment O_2 influx in all seasons, nearly double Bare rates for all sampling times except October and June, when the difference was less pronounced. Sediment O_2 flux was significantly different across sites and month (p<0.0005), but there was no interaction effect (p=1.58). Row sites consistently had intermediate O_2 fluxes between Oyster and Bare, and were statistically different from both (p<0.0005 for Oyster, and p=0.039 for Bare). The farm sites (Oyster and Row, collectively) had peak O_2 influx in April, exceeding -5,000 µmol O_2 m^{-2} h^{-1} and -3,100 µmol O_2 m^{-2} h^{-1} respectively, whereas the Bare rate for the same period was -2,300 µmol O_2 m^{-2} h^{-1}. The final sampling in June had lower than expected O_2 fluxes within the farm, compared to the previous summer and spring rates. This may have been caused by the farmer reorienting the farm in May, which could have disrupted the pre-existing sediment structure. Other measured processes, however, including denitrification, DNRA, and nutrient fluxes, were similar in magnitude to the previous summer samplings.

Benthic NH_4^+ flux to the water column was significantly enhanced at the farm sites relative to the Bare site (p<0.0005 for Oyster and p=0.005 for Row), and summer fluxes at Oyster sites reached 935 µmol m^{-2} h^{-1} (Figure 4A). Ammonium flux also differed significantly across months, and there was a significant site*sampling time interaction effect, with greater seasonal enhancement at the farm sites

(p<0.0005). Bare sites had undetectable to low NH_4^+ flux during fall through spring, and small fluxes (<72 µmol m^{-2} h^{-1}) in the summer months.

Nitrate flux was consistently low or below instrument detection and there was no significant difference between seasons or sites (p<0.289) (Figure 4B). When detectable, average flux was either not significantly different from 0 or directed into the sediment (maximum -10 µmol m^{-2} h^{-1}). N_2O fluxes measured in April were also consistently small and negative (directed into the sediment), ranging from -0.042 to -0.067 (± <0.014) µmol m^{-2} h^{-1}. Rates were not significantly different among sites (p=0.405).

SRP flux followed patterns similar to NH_4^+, with consistently low fluxes at Bare sites, and significant seasonal (summer) enhancement within the farm (p=0.003 for the interaction effect) (Figure 4C). All sites had undetectable fluxes in January, and the flux at farm sites increased in June to 37 and 148 µmol m^{-2} h^{-1} for Row and Oyster, respectively. Overall, fluxes were significantly different both across sites and sampling time (p<0.0005 and p=0.001, respectively).

Denitrification and DNRA

Denitrification (D14) was relatively low during all months, but there were significant differences across sampling time and site, as well as a significant interaction effect (p<0.0005) (Figure 5A). Denitrification was consistently higher within the farm, except in June when all three sites had very low rates (<2 µmol N m^{-2} h^{-1}). Oyster sites were significantly different from both Row and Bare (p<0.0005), and although Row sites were also typically enhanced above Bare, Row and Bare were not significantly different (p=0.240). Rates were significantly higher in the cooler months (p<0.0005 for January and April), when maximum Oyster rates reached 9.6 (±2.0) to 19.2 (±1.4) µmol N m^{-2} h^{-1}.

Denitrification of the added $^{15}NO_3$ (D15) mirrored the D14 pattern both seasonally and by site, although rates were on average six times higher. The maximum farm D15 occurred at Oyster sites in April, reaching 110.7 (±1.0) µmol N m^{-2} h^{-1}. For comparison, D15 at Row sites was 37.4 (±9.4) and at Bare

sites was 17.8 (±4.1) µmol N m^{-2} h^{-1}. D15 in July, August, October, and June were much lower at all sites, ranging from 4.2 to 14.2 µmol N m^{-2} h^{-1} within the farm (both values at Oyster sites), and 4.4 to 7.2 µmol N m^{-2} h^{-1} at the Bare site. As with D14, D15 was statistically different across sites and by interaction between site and sampling time (p<0.0005), as well as across sampling times, with significantly higher rates in January and April (p<0.001).

Despite enhanced denitrification within the farm, DE was significantly lower within the farm relative to Bare sites, as a result of the enhanced NH_4^+ fluxes (p=0.001 for Row and p<0.0005 for Oyster). The highest DE within the farm occurred in April when denitrification was at a maximum and NH_4^+ flux relatively low, reaching 9% (±4%) and 28% (±7%) for Oyster and Bare, respectively. In summer, however, the maximum DE was <0.01% (±0.00%) for both sites. In comparison, the Bare site had DE of 69% (±31%) in January due to negligible or negative NH_4^+ fluxes. The Bare site DE was highly variable in summer due to very low rates of both denitrification and benthic NH_4^+ and NO_3^- fluxes, ranging from 50% (±29%) in August to 0.02% (±0.01%) in June. Note that these values do not include dissolved organic N fluxes, which can be significant and highly variable depending on environmental conditions. Including DON flux would further reduce the calculated denitrification efficiency rate.

DNRA rates were generally higher than denitrification, and ranged from <1 to 40.3 µmol N m^{-2} h^{-1}. Similar to denitrification, DNRA at the farm sites were consistently and significantly higher than Bare sites (p<0.0005 for both Oyster and Row), but there was no interaction effect with sampling time (p=0.352) and no clear seasonal trend (Figure 5B). DNRA accounted for at least 70% of total NO_3^- reduction (DNRA plus denitrification) for most sampling dates and sites (Figure 5C). In July, October, and June, DNRA exceeded >90% of total NO_3^- reduction. Exceptions to DNRA dominance occurred only in August for Bare and Row sites (due to relatively low DNRA) and in April for Oyster sites (due to relatively high denitrification). During these times, DNRA and denitrification were approximately equal. As both

DNRA and denitrification were generally enhanced within the farm, there was no difference in the contribution of DNRA to total NO_3^- reduction across sites (p=0.58).

Discussion

Enhanced but limited denitrification within the farm

Enhanced denitrification in oyster ecosystems is predicted based on increased biodeposition of organic C and N, which can support denitrifying microbes either directly through C inputs when NO_3^- concentrations are high or indirectly via coupled nitrification-denitrification when NO_3^- is limited (Newell 2004). Observations in coastal ecosystems in general support this hypothesis, as denitrification is often positively correlated with OM deposition (Babbin et al. 2014). However, existing data from oyster aquaculture settings have not shown enhanced denitrification within farms (Kellogg et al. 2014). The only previously published study measuring denitrification at an oyster aquaculture site found an insignificant trend of enhanced denitrification in core incubations, and inhibited denitrification in slurry incubations (Higgins et al. 2013). This study, on the other hand, found a clear trend of denitrification enhancement within the farm during most months, and farm rates were on average 250% (Row) to 370% (Oyster) higher than at the Bare site. We did not measure biodeposition, but rates were clearly higher within the farm relative to Bare sites, as mounds of accumulated material were present under oyster racks. Sediment C and N were also highest at Oyster sites, followed by Row and Bare sites, indicating higher C and N availability. Denitrification followed the sediment C and N pattern, with highest rates at the Oyster sites, followed by Row and Bare, respectively.

Although denitrification was enhanced within the farm, absolute rates were very low during all seasons. Denitrification at our sites ranged from <1 μmol m^{-2} h^{-1} to 19.2 μmol N m^{-2} h^{-1}, whereas rates in other estuarine systems are often measured up to 250 μmol N m^{-2} h^{-1} (Seitzinger 1988; Cornwell et al. 1999), and seasonal rates in oyster reefs have been recorded as high as 1600 μmol m^{-2} h^{-1} (Kellogg et al.

2013). Rates at our site were likely limited by inhibited nitrification caused by anoxic sediment conditions. Ambient NO_3^- at the site is very low (<1 μM on all measured dates), so denitrification is largely dependent on coupled nitrification-denitrification. Although IPT enables calculation of the relative contributions of water column-derived versus coupled nitrification-denitrification, we did not calculate these values because of a) methodological concerns about the validity of the equations (Middelburg et al. 1996), and b) the ambient NO_3^- concentration, which is required for the calculations, was at or below the analytical detection limit. However, given this low ambient concentration and undetectable NO_3^- fluxes in some months, it is clear that denitrification at our site relies significantly on coupled nitrification-denitrification.

Nitrate limitation was evident at the farm from several indicators. First, the observed denitrification follows typical seasonal nitrification trends, with highest rates in winter and spring, suggesting that denitrification was controlled by NO_3^- availability. Nitrification is often observed to peak in spring before enhanced microbial respiration in summer depletes sediment O_2 (Jenkins and Kemp 1984). In addition to the seasonal trend, NO_3^- and N_2O fluxes were almost exclusively negative at all sites, indicating that NO_3^- consuming processes (e.g. denitrification and DNRA) exceed sediment NO_3^- availability (Koike and Hattori 1975; Kieskamp et al. 1991). Finally, limited NO_3^- availability was indicated by greatly enhanced denitrification stimulated by the ^{15}N addition: the D15 rate (denitrification of the amended $^{15}NO_3^-$) for all sites was on average six times higher than the calculated in situ rate. Thus, the sediment denitrifying communities at all sites did not appear to be C limited, but rather NO_3^- limited. It is interesting to note that while the measured denitrification rates were low, the enhanced D15 suggests that denitrification in the farm may be effective at removing pulses of NO_3^- during storm events. The Bare sites may have been limited not only by low nitrification, but by N availability in general, since sediment N content was very low, as was NH_4^+ flux during fall through spring.

Sediment anoxia inhibits coupled nitrification-denitrification and enhances nutrient efflux

Limited nitrification in the farm is a direct result of sediment anoxia, likely caused by high OM loading. Sediment anoxia was indicated by high SOD at the farm sites, especially at Oyster sites, which were on average nearly twice that of Bare sites. Anoxia in farm sediments was also apparent during the IPT slurrying process, when the O_2 concentration of the sediment plus water mixture fell sharply. For example, in the April IPT incubation, water column concentrations at the end of the incubations were on average 60% saturation, but after slurrying, O_2 dropped to an average of 5% in the Oyster cores, compared to 22% at Row sites and 37% in the Bare cores. The observed reduction in the Oyster cores exceeded the expected value based on water column and porewater mixing, even assuming completely anoxic porewater. This O_2 depletion was assumed to be the result of high concentrations of reduced inorganic species like sulfides and iron(II), which stripped O_2 from the slurry via geochemical oxidation. The accumulation of such reduced species in the Oyster sites, and to a lesser extent the Row sites, implies that OM mineralization is highly dependent on iron and/or sulfur as electron acceptors, instead of O_2 at those sites. In addition to indicating anoxia, reduced sulfur species can also directly inhibit nitrification (Joye and Hollibaugh 1995), and along with reduced iron species, can lead to release of adsorbed SRP (Roden and Edmonds 1997; Heijs et al. 2000). Significant SRP fluxes from the farm sediments in summer (up to 148 μmol m^{-2} h^{-1} at Oyster sites) thus further indicated accumulation of these reduced species. Similar rates of SRP release have been observed in other bivalve aquaculture studies where sediment anoxia was prevalent. (Nizzoli et al. 2007; Carlsson et al. 2012).

The conceptual model shown in Figure 1 suggests that denitrification should be enhanced at low to moderate oyster densities, and limited or inhibited at higher densities when excessive OM loading induces sediment anoxia and thus inhibits nitrification (Newell 2004). The oyster density in this model is not explicitly quantified, but is likely to vary with site conditions like hydrodynamics and sediment qualities. We expected enhanced nitrification-denitrification because the oyster density at our site was

low compared to natural reef densities and moderate for commercial farm densities. The stocking density at the farm was 140 oysters m^{-2}, and the harvest density half that. Commercial oyster farms average 100-200 oysters m^{-2}, with high densities up to 500 oysters m^{-2} (Ferreira et al. 2007; STAC 2013; JM Rose et al. 2015). The maximum density at our farm could be high in some locations, for example up to 600 individual market-sized oysters m^{-2} in bags for that age class. However, natural oyster reefs can support even higher densities, from 1,000 to >3,000 oysters m^{-2} (Schulte et al. 2009; Smyth et al. 2015), and Smyth et al. (2015) found that denitrification increased with oyster density up to 2,400 oysters m^{-2}. Although the density at our farm was on the low end of reef and aquaculture densities, OM loading was nonetheless apparently sufficient to induce sediment anoxia and limit coupled nitrification-denitrification. The differences in density thresholds for denitrification may depend to some degree on hydrodynamics or cultivation type, as higher flow locations and/or bivalves grown higher in the water column may result in more dispersed biodeposits, allowing for higher densities without inducing sediment anoxia.

We expected to find the highest denitrification rates in the Row sites due to regular perturbation and oxygenation of the reduced sediment. However, denitrification at the Row sites was not significantly different from Oyster during the summer sampling dates, and was significantly lower than Oyster during the other three seasons. The Row cores were not as obviously reduced as the Oyster cores, as indicated by O_2 depletion during slurrying, but they were nonetheless reduced enough to indicate anoxic sediment. Thus, denitrification at the Row sites also appeared to be limited by inhibited nitrification.

In addition to high OM loading, limited nitrification could also be sustained by environmental factors within the farm. For example, smaller average sediment grain size (i.e., higher silt and clay content) in the farm compared to the Bare site could exacerbate sediment anoxia. Small grain size, in general, can physically retain OM more so than coarser grained sediments (Gray and Elliott 2009). As a

result, finer grained sediment combined with high OM loading can support microbial metabolism that leads to sediment anoxia and sulfide accumulation (Martinez-Garcia et al. 2015). Low concentrations of benthic microalgae (BMA) at all sites could also maintain anoxic sediment conditions. In low O_2 sediments like those in the farm, BMA can stimulate nitrification by creating localized oxic conditions (Risgaard-Petersen et al. 1994; Christensen et al. 2003; Dunn et al. 2012). However, at our sites, chlorophyll *a* concentrations were less than 40 mg m^{-2} during both seasons measured. This is relatively low compared to concentrations in other coastal systems, which can be up to 800 mg m^{-2} (Underwood and Kromkamp 1999; An and Joye 2001). High turbidity from frequent work at this and other farms in the inlet may contribute to such low concentrations (Underwood and Kromkamp 1999; Dunn et al. 2012). It should be noted that BMA has also been associated with *lowering* denitrification rates through competition for NO_3^-, however this is typically observed in situations where denitrification is driven by water column, not nitrification-derived NO_3^- (Risgaard-Petersen et al. 1994).

Because coupled nitrification-denitrification was limited, most of the benthic N flux consisted of regenerated NH_4^+. On average, NH_4^+ accounted for 97% to 99% of the measured N fluxes at Row and Oyster sites, respectively. The absolute rates of NH_4^+ flux from the Oyster sites were very high, reaching over 900 µmol m^{-2} h^{-1} in summer, which are among the highest rates in the published literature. NH_4^+ flux from bivalve aquaculture typically range from 100 to 1000 µmol m^{-2} h^{-1} (Nizzoli et al. 2006; Carlsson et al. 2012; Higgins et al. 2013). However, one study at a floating mussel farm in operation for only six months found relatively low rates ranging from <-700 µmol m^{-2} h^{-1} (influx) to 200 µmol m^{-2} h^{-1} (Holmer et al. 2015). Thus, farm age and accumulation of sediment OM may be a factor determining NH_4^+ flux. The study farm had been in operation for only four years, which was apparently long enough for OM to accumulate sufficiently for year-round NH_4^+ flux. Ammonium flux was negligible at the Bare site in fall through spring, but both farm sites had significant positive fluxes in all seasons, and the minimum Oyster flux in winter exceeded the maximum summer flux at the Bare site. This significant, year-round

flux from the farm could be an important ecological consideration due to both its magnitude and seasonal alteration of water column nutrients.

Although denitrification was enhanced within the farm, the relatively larger increase in NH_4^+ flux resulted in decreased DE at the farm sites. Reduced DE within the farm implies that farm sediments denitrify relatively less N per unit of N deposition than sites outside of the farm. As a result, although absolute rates in the farm were enhanced, it is possible that total denitrification at the basin-scale would be reduced if deposition is enhanced within the farm. Low DE is often associated with excessive OM loading, and has been observed in commercial bivalve farms with similar anoxic sediment conditions (Eyre and Ferguson 2009; Carlsson et al. 2012). The observed farm DE values (annual average of 4% for Oyster and 11% for Bare) were lower than one of the original, and frequently cited, DE estimates in oyster-impacted sediments, which found DE over 20% in laboratory experiments (Newell et al. 2002).

The significantly enhanced NH_4^+, and to a lesser extent SRP, to the water column raises concerns about eutrophication and related impacts. In poorly flushed systems, similar nutrient fluxes from bivalve farms can cause excessive algal growth, subsequent decay, and water column anoxia (Bartoli et al. 2001). However, Cherrystone has a high tidal prism (approximately ½ of the inlet volume per day), and eutrophication symptoms caused by aquaculture are not currently evident. Ambient nutrient conditions (both N and P) remained low (<2 μM) throughout the study, and a recent study conducted within the inlet found that 20 to 77% of the NH_4^+ emitted from clam aquaculture sediments may be assimilated by macroalgae (Murphy et al. 2015). This macroalgae can occur as dense mats on aquaculture structures, especially those used in clam farming, but it is regularly removed during farm maintenance, and believed to be largely exported from the inlet during daily tidal flushing (Mark Brush, personal communication). SRP is less effectively assimilated by macroalgae (Murphy et al. 2015), so the enhanced fluxes are more likely to be directly exported from the inlet. Thus, in this system, rapid assimilation of nutrients by primary producers, removal of macroalgae during farm maintenance, and sufficient tidal

flushing appear to maintain water quality despite high rates of nutrient regeneration from aquaculture sediment.

DNRA dominates nitrate reduction

This study is the first to provide in situ DNRA rates for oyster aquaculture, and we found that DNRA dominance may have further contributed to limited denitrification. Across all seasons and cores, DNRA accounted for an average of 79% of total NO_3^- reduction (i.e., denitrification and DNRA cumulatively). DNRA contribution to NO_3^- reduction varies widely in coastal environments, ranging from insignificance (0%) to complete dominance (100%) (Megonigal et al. 2004; Burgin and Hamilton 2007; Giblin et al. 2013). However, many studies of aquaculture systems, like ours, have found DNRA to be the dominant NO_3^- reduction pathway and/or occur at high rates (Gilbert et al. 1997; Christensen et al. 2000; Nizzoli et al. 2006). These data support the hypothesis that previously understudied N processes like DNRA may be more significant than denitrification in some settings, and that denitrification may be overemphasized as a N pathway in coastal ecosystems (Burgin and Hamilton 2007).

The environmental conditions driving DNRA preference over denitrification are still unclear, but proposed factors include sediment OM content (Song et al. 2014), the relative availability of organic C to NO_3^- (Tiedje et al., 1983; Megonigal et al., 2004 and references therein), the NO_2^- to NO_3^- ratio (Kraft et al. 2014), salinity (Giblin et al. 2010), and temperature (Kelly-Gerreyn et al. 2001). At our site, enhanced deposition of highly labile biodeposits within the farm, in combination with low NO_3^- availability could explain the high rates. DNRA has been shown to dominate with these conditions in laboratory tests (Kraft et al. 2014). DNRA dominance is also often associated with highly reduced, sulfidic conditions like those at our site (Joye and Hollibaugh 1995; Brunet and Garcia-Gil 1996; Gardner and McCarthy 2009). However, some studies have shown denitrification dominance even in high sulfide conditions (Behrendt et al. 2013; Kraft et al. 2014), so the association of DNRA with sulfides may be correlational and not

causal. Elevated delivery of highly labile OM could lead to both elevated C availability and reduced, sulfidic conditions. Similarly, studies focused on temperature have indicated that denitrification is preferred over DNRA only at low temperatures, or within a narrow temperature range of 14°C and 17°C (Kelly-Gerreyn et al. 2001). While denitrification was enhanced at this temperature range in our study (in April), DNRA was still the dominant NO_3^- reduction pathway. Thus, temperature may have been a factor in absolute rates, but was not a strong control on DNRA.

While DNRA was enhanced at the farm sites relative to the Bare sties, similar to denitrification, absolute rates were low. DNRA contribution to total NH_4^+ flux was therefore minimal. In summer, when NH_4^+ fluxes were highest, DNRA accounted for <4% of benthic NH_4^+ flux for the farm sites, and 15% for the Bare sites. Thus, most of the NH_4^+ flux is likely the product of direct mineralization of highly labile material, as opposed to resulting from DNRA.

Limited spatial impact

N cycling—as measured by denitrification, DNRA, and NH_4^+ flux—was significantly enhanced within the farm, but was spatially limited to the Oyster sites. Measurements of these processes at Row sites, located less than 1 m from the nearest oyster bag, were intermediate between Oyster and Bare, and in most instances were not significantly different from Bare sites. Furthermore, a 60-m transect radiating from the farm boundary found OM was higher near the farm, but stabilized beyond 40 m, near the selected Bare site (data not shown). The similarity between Row and Bare sites, as well as the proximity of a constant OM zone, indicate that impact from the oysters was spatially limited. Small footprints are common in bivalve aquaculture, and impacted sediment properties are typically limited to tens of meters beyond farm boundaries (Chamberlain et al. 2001; Callier et al. 2006; Forrest and Creese 2006; Giles et al. 2009). Similarly, Rumrill and Poulton (2004) found that seagrass density in an oyster farm did not differ from reference sites if oyster rows were spaced by only 5 feet.

Site-specific conditions such as hydrodynamics (Giles et al. 2009) and water depth (Wilson and Vopel 2015) can influence the benthic footprint area, as deeper or higher current sites can disperse (and thus dilute) biodeposits over larger areas. Cultivation method is an important factor in this regard, as floating-type cultivation increases water depth relative to near-bottom methods like that in our study. The assumed dilution of biodeposits at floating-type farms may explain why previous studies of denitrification in oyster aquaculture found no significant difference between farm and control sites (Holyoke 2008; Higgins et al. 2013). While the farm studied by Higgins et al. (Higgins et al. 2013) supported oyster density higher than ours (236 oysters m^{-2}), oysters were cultivated at >1.5 m above the sediment surface, so biodeposits were likely dispersed more effectively. Similarly, Crawford et al. (2003) found no significant benthic impact in terms of redox potential, sulfide concentration, or C content in a study of longline (off-bottom) mussel and oyster cultivation. The near-bottom, rack and bag method analyzed in our study concentrates biodeposits in a relatively small area under oyster bags, limiting the farm footprint, but contributing to reduced, anoxic conditions that limit denitrification and enhance NH_4^+ and SRP flux.

Conclusions

Building on a conceptual model predicting enhanced denitrification caused by oyster biodeposition (Figure 1) (Newell 2004), we provide the first field verification that benthic denitrification is enhanced in a *Crassostrea virginica* oyster farm. However, absolute denitrification rates remained low, and maximum denitrification in the farm was only 19.2 µmol N m^{-2} h^{-1}. Denitrification was likely limited by NO_3^-, a result of low ambient concentration and inhibited nitrification caused by sediment anoxia. Stocking density in the farm was typical of commercial oyster farms, yet OM loading was apparently sufficient to deplete sediment O_2. As a result, direct NH_4^+ efflux was the dominant N pathway in the farm, accounting for an average of 97% to 99% of total benthic N flux (N_2, NO_3^-, and NH_4^+) at Row and

Oyster sites, respectively. DE was thus lower in the farm relative to the Bare sites. DNRA may also have contributed to low denitrification rates, as it accounted for an average of 70% of NO_3^- reduction at all sites.

The spatial extent of the enhanced fluxes and processes was extremely limited, with highest rates directly under oysters, and rates more similar to Bare sites in between oyster rows. These findings indicate that the potential for greatly enhanced denitrification at oyster aquaculture sites may be overstated, at least at sites where denitrification depends on coupled nitrification. Future studies should be conducted at oyster farms in locations with higher concentrations of water column NO_3^- to assess whether or not such conditions would support higher denitrification rates.

Acknowledgements

This research was supported by grants from Virginia Sea Grant's Graduate Student Fellowship program and a student grant from the Virginia Water Resources Research Center. I would like to thank Michael Pace at University of Virginia for providing feedback, support, and lab materials. I am also grateful to Lillian Aoki, Marie Lise Delgard, Matthew Oreska, Meigan McManus, and Devin Rowell for their assistance in the laboratory and field.

References

An, S, and SB Joye. 2001. Enhancement of coupled nitrification-denitrification by benthic photosynthesis in shallow estuarine sediments. *Limnology and Oceanography* 46: 62–74.

Babbin, AR, RG Keil, AH Devol, and BB Ward. 2014. Organic matter stoichiometry, flux, and oxygen control nitrogen loss in the ocean. *Science* 344: 406–408. doi:10.1126/science.1248364.

Bartoli, M, D Nizzoli, P Viaroli, E Turolla, G Castaldelli, EA Fano, and R Rossi. 2001. Impact of Tapes philippinarum farming on nutrient dynamics and benthic respiration in the Sacca di Goro. *Hydrobiologia* 455: 203–212.

Behrendt, A, D de Beer, and P Stief. 2013. Vertical activity distribution of dissimilatory nitrate reduction in coastal marine sediments. *Biogeosciences* 10: 7509–7523. doi:10.5194/bg-10-7509-2013.

Bouwman, AF, M Pawłowski, C Liu, AHW Beusen, SE Shumway, PM Glibert, and CC Overbeek. 2011. Global Hindcasts and Future Projections of Coastal Nitrogen and Phosphorus Loads Due to Shellfish and Seaweed Aquaculture. *Reviews in Fisheries Science* 19: 331–357. doi:10.1080/10641262.2011.603849.

Brunet, RC, and LJ Garcia-Gil. 1996. Sulfide-induced dissimilatory nitrate reduction to ammonia in anaerobic freshwater sediments. *FEMS Microbiology Ecology* 21: 131–138.

Burgin, AJ, and SK Hamilton. 2007. Have we overemphasized the role of denitrification in aquatic ecosystems ? A review of nitrate removal pathways. *Frontiers in Ecology and the Environment* 5: 89–96.

Callier, MD, AM Weise, CW McKindsey, and G Desrosiers. 2006. Sedimentation rates in a suspended mussel farm (Great-Entry Lagoon, Canada): biodeposit production and dispersion. *Marine Ecology Progress Series* 322. Inter-Research: 129–141.

Carlsson, MS, P Engström, O Lindahl, L Ljungqvist, JK Petersen, L Svanberg, and M Holmer. 2012. Effects of mussel farms on the benthic nitrogen cycle on the Swedish west coast. *Aquaculture Environment Interactions* 2: 177–191. doi:10.3354/aei00039.

Carmichael, RH, W Walton, and H Clark. 2012. Bivalve-enhanced nitrogen removal from coastal estuaries. *Canadian Journal of Fisheries and Aquatic Sciences* 69: 1131–1149. doi:10.1139/F2012-057.

Chamberlain, Jn, TF Fernandes, P Read, TD Nickell, and IM Davies. 2001. Impacts of biodeposits from suspended mussel (Mytilus edulis L.) culture on the surrounding surficial sediments. *ICES Journal of Marine Science: Journal du Conseil* 58. Oxford University Press: 411–416.

Chapelle, A, A Ménesguen, JM Deslous-Paoli, P Souchu, N Mazouni, A Vaquer, and B Millet. 2000. Modelling nitrogen, primary production and oxygen in a Mediterranean lagoon. Impact of oysters farming and inputs from the watershed. *Ecological modelling* 127. Elsevier: 161–181.

Christensen, PB, RN Glud, T Dalsgaard, and P Gillespie. 2003. Impacts of longline mussel farming on oxygen and nitrogen dynamics and biological communities of coastal sediments. *Aquaculture* 218: 567–588.

Christensen, PB, S Rysgaard, NP Sloth, T Dalsgaard, and S Schwaerter. 2000. Sediment mineralization, nutrient fluxes, denitrification and dissimilatory nitrate reduction to ammonium in an estuarine fjord with sea cage trout farms. *Aquatic Microbial Ecology* 21: 73–84.

Cornwell, JC, WM Kemp, and TM Kana. 1999. Denitrification in coastal ecosystems: methods, environmental controls, and ecosystem level controls, a review. *Aquatic Ecology* 33: 41–54.

Correll, DL. 1998. The role of phosphorus in the eutrophication of receiving waters: A review. *Journal of Environmental Quality* 27. American Society of Agronomy, Crop Science Society of America, and Soil Science Society of America: 261–266.

Crawford, CM, CKA Macleod, and IM Mitchell. 2003. Effects of shellfish farming on the benthic environment. *Aquaculture* 224: 117–140. doi:10.1016/S0044-8486(03)00210-2.

Dame, RF, JD Spurrier, and RG Zingmark. 1992. In situ metabolism of an oyster reef. *Journal of Experimental Marine Biology and Ecology* 164. Elsevier: 147–159.

Dunn, RJK, DT Welsh, M Jordan, NJ Waltham, CJ Lemckert, and PR Teasdale. 2012. Benthic metabolism and nitrogen dynamics in a sub-tropical coastal lagoon: Microphytobenthos stimulate nitrification and nitrate reduction through photosynthetic oxygen evolution. *Estuarine, Coastal and Shelf Science* 113. Elsevier Ltd: 272–282. doi:10.1016/j.ecss.2012.08.016.

Eyre, BD, and AJP Ferguson. 2009. Denitrification efficiency for defining critical loads of carbon in shallow coastal ecosystems. *Hydrobiologia* 629: 137–146. doi:10.1007/s10750-009-9765-1.

Ferreira, JG, AS Hawkins, and SB Bricker. 2007. Management of productivity, environmental effects and profitability of shellfish aquaculture — the Farm Aquaculture Resource Management (FARM) model. *Aquaculture* 264: 160–174. doi:10.1016/j.aquaculture.2006.12.017.

Forrest, BM, and RG Creese. 2006. Benthic impacts of intertidal oyster culture, with consideration of taxonomic sufficiency. *Environmental Monitoring and Assessment* 112. Springer: 159–176.

Gardner, WS, and MJ McCarthy. 2009. Nitrogen dynamics at the sediment–water interface in shallow, sub-tropical Florida Bay: why denitrification efficiency may decrease with increased eutrophication. *Biogeochemistry* 95. Springer: 185–198.

Giblin, AE, CR Tobias, B Song, N Weston, GT Banta, and VH Rivera-Monroy. 2013. The importance of dissimilatory nitrate reduction to ammonium (DNRA) in the nitrogen cycle of coastal ecosystems. *Oceanography* 26: 124–131.

Giblin, AE, NB Weston, GT Banta, J Tucker, and CS Hopkinson. 2010. The effects of salinity on nitrogen losses from an oligohaline estuarine sediment. *Estuaries and Coasts* 33. Springer: 1054–1068.

Gilbert, F, P Souchu, M Bianchi, and PC Bonin. 1997. Influence of shellfish farming activities on nitrification, nitrate reduction to ammonium and denitrification at the water-sediment interface of the Thau lagoon, France. *Marine Ecology Progress Series* 151: 143–153.

Giles, H, N Broekhuizen, KR Bryan, and CA Pilditch. 2009. Modelling the dispersal of biodeposits from mussel farms: The importance of simulating biodeposit erosion and decay. *Aquaculture* 291. Elsevier B.V.: 168–178. doi:10.1016/j.aquaculture.2009.03.010.

Glass, GV, PD Peckham, and JR Sanders. 1972. Consequences of failure to meet assumptions underlying the fixed effects analyses of variance and covariance. *Review of educational research*. JSTOR: 237–288.

Gray, JS, and M Elliott. 2009. *Ecology of marine sediments: from science to management*. Oxford University Press.

Heijs, SK, R Azzoni, G Giordani, HM Jonkers, D Nizzoli, P Viaroli, and H van Gemerden. 2000. Sulfide-induced release of phosphate from sediments of coastal lagoons and the possible relation to the disappearance of Ruppia sp. *Aquatic Microbial Ecology* 23: 85–95.

Heisler, J, PM Glibert, JM Burkholder, DM Anderson, and W Cochlan. 2008. Eutrophication and harmful algal blooms : A scientific consensus. *Harmful Algae* 8: 3–13.

Higgins, CB, C Tobias, MG Piehler, AR Smyth, RF Dame, K Stephenson, and BL Brown. 2013. Effect of aquacultured oyster biodeposition on sediment N2 production in Chesapeake Bay. *Marine Ecology Progress Series* 473: 7–27. doi:10.3354/meps10062.

Holmer, M, SW Thorsen, MS Carlsson, and PJ Kjerulf. 2015. Pelagic and Benthic Nutrient Regeneration Processes in Mussel Cultures (Mytilus edulis) in a Eutrophic Coastal Area (Skive Fjord, Denmark). *Estuaries and Coasts* 38. doi:10.1007/s12237-014-9864-8.

Holyoke, RR. 2008. Biodeposition and Biogeochemical Processes in Shallow, Mesohaline Sediments of Chesapeake Bay. Ph.D. dissertation. University of Maryland, College Park, MD.

Jenkins, MC, and WM Kemp. 1984. The coupling of nitrification and denitrification in two estuarine sediments1, 2. *Limnology and Oceanography* 29. Wiley Online Library: 609–619.

Joye, SB, and JT Hollibaugh. 1995. Influence of Sulfide Inhibition of Nitrification on Nitrogen Regeneration in Sediments. *Science* 275: 623–625.

Kellogg, ML, J Cornwell, M Owens, and K Paynter. 2013. Denitrification and nutrient assimilation on a restored oyster reef. *Marine Ecology Progress Series* 480: 1–19. doi:10.3354/meps10331.

Kellogg, ML, AR Smyth, MW Luckenbach, RH Carmichael, BL Brown, JC Cornwell, MF Piehler, MS Owens, DJ Dalrymple, and CB Higgins. 2014. Use of oysters to mitigate eutrophication in coastal waters. *Estuarine, Coastal and Shelf Science* 151. Elsevier Ltd: 156–168. doi:10.1016/j.ecss.2014.09.025.

Kelly-Gerreyn, BA, M Trimmer, and DJ Hydes. 2001. A diagenetic model discriminating denitrification

and dissimilatory nitrate reduction to ammonium in a temperate estuarine sediment. *Marine Ecology Progress Series* 220. Inter-Research: 33–46.

Kieskamp, WM, L Lohse, E Epping, and W Helder. 1991. Seasonal variation in denitrification rates and nitrous oxide fluxes in intertidal sediments of the western Wadden Sea. *Marine Ecology Progress Series* 72: 145–151.

Koike, I, and A Hattori. 1975. Energy yield of denitrification: an estimate from growth yield in continuous cultures of Pseudomonas denitrificans under nitrate-, nitrite-and nitrous oxide-limited conditions. *Microbiology* 88. Soc General Microbiol: 11–19.

Kraft, B, HE Tegetmeyer, R Sharma, MG Klotz, TG Ferdelman, RL Hettich, JS Geelhoed, and M Strous. 2014. The environmental controls that govern the end product of bacterial nitrate respiration. *Science* 345: 676–679. doi:10.1126/science.1254070.

Kuschner, MA. 2015. A model of carrying capacity and ecosystem impacts in a large-scale, bivalve dominated agro-ecosystem: hard clam aquaculture in Cherrystone Inlet, VA. Virginia Institute of Marine Science, College of William and Mary.

Lorenzen, CJ. 1965. Determination of chlorophyll and phaeopigments: spectrophotometric equations. *Limnology and Oceanography* 12.2: 343–346.

Lunstrum, A, and L Aoki. 2015. Oxygen interference with membrane inlet mass spectrometry may overestimate denitrification rates calculated with the isotope pairing technique. *In preparation*.

Martinez-Garcia, E, MS Carlsson, P Sanchez-Jerez, JL Sánchez-Lizaso, C Sanz-Lazaro, and M Holmer. 2015. Effect of sediment grain size and bioturbation on decomposition of organic matter from aquaculture. *Biogeochemistry* 125: 133–148. doi:10.1007/s10533-015-0119-y.

Mazouni, N, JC Gaertner, JM Deslous-Paoli, S Landrein, and M Geringer d'Oedenberg. 1996. Nutrient and oxygen exchanges at the water-sediment interface in a shellfish farming lagoon (Thau, France). *Journal of Experimental Marine Biology and Ecology* 205. Elsevier: 91–113.

Megonigal, JP, ME Hines, and PT Visscher. 2004. Anaerobic Metabolism: Linkages to Trace Gases and Aerobic Processes. In *Biogeochemistry*, ed. William H. Schlesinger, 317–424. Oxford, UK: Elsevier-Pergamon.

Middelburg, JJ, K Soetaert, and PMJ Herman. 1996. Evaluation of the nitrogen isotope-pairing method for measuring benthic denitrification: A simulation analysis. *Limnology and Oceanography* 41: 1839–1844.

Murphy, A, IC Anderson, and M Luckenbach. 2015. Enhanced nutrient regeneration at commercial hard clam (Mercenaria mercenaria) beds and the role of macroalgae. *Marine Ecology Progress Series* 530: 135–151. doi:10.3354/meps11301.

Newell, RIE. 2004. Ecosystem influences of natural and cultivated populations of suspension-feeding bivalve molluscs: a review. *Journal of Shellfish Research* 23: 51–61.

Newell, RIE, JC Cornwell, and MS Owens. 2002. Influence of simulated bivalve biodeposition and microphytobenthos on sediment nitrogen dynamics: A laboratory study. *Limnology and Oceanography* 47. Wiley Online Library: 1367–1379.

Nielsen, LP. 1992. Denitrification in sediment determined from nitrogen isotope pairing. *FEMS Microbiology Letters* 86. The Oxford University Press: 357–362.

Nixon, SW. 1995. Coastal marine eutrophication: a definition, social causes, and future concerns. *Ophelia* 41. Taylor & Francis: 199–219.

Nizzoli, D, M Bartoli, and P Viaroli. 2007. Oxygen and ammonium dynamics during a farming cycle of the bivalve Tapes philippinarum. *Hydrobiologia* 587: 25–36. doi:10.1007/s10750-007-0683-9.

Nizzoli, D, DT Welsh, EA Fano, and P Viaroli. 2006. Impact of clam and mussel farming on benthic metabolism and nitrogen cycling, with emphasis on nitrate reduction pathways. *Marine Ecology Progress Series* 315: 151–165. doi:10.3354/meps315151.

Petersen, JK, K Timmermann, M Carlsson, M Holmer, M Maar, and O Lindahl. 2012. Mussel farming can be used as a mitigation tool--a reply. *Marine pollution bulletin* 64: 452–4; author reply 455–6. doi:10.1016/j.marpolbul.2011.11.027.

Risgaard-Petersen, N, RL Meyer, MC Schmid, Mike SM Jetten, A Enrich-Prast, S Rysgaard, and NP Revsbech. 2004. Anaerobic ammonium oxidation in an estuarine sediment. *Aquatic Microbial Ecology* 36: 293–304.

Risgaard-Petersen, N, and S Rysgaard. 1995. Nitrate reduction in sediments and waterlogged soil measured by 15N techniques. In *Methods in applied Soil microbiology*, 287–310.

Risgaard-Petersen, N, S Rysgaard, and LP Nielsen. 1994. Diurnal variation of denitrification and nitrification in sediments colonized by benthic microphytes. *Limnology and Oceanography* 39: 573–579.

Roden, EE, and JW Edmonds. 1997. Phosphate mobilization in iron-rich anaerobic sediments: microbial Fe(III) oxide reduction versus iron-sulfide formation. *Archiv für Hydrobiologie* 193: 347–378.

Rose, J, SB Bricker, M Tedesco, and G Wikfors. 2014. A role for shellfish aquaculture in coastal nitrogen management. *Environmental Science & Technology*. doi:10.1021/es4041336.

Rose, JM, SB Bricker, and JG Ferreira. 2015. Comparative analysis of modeled nitrogen removal by shellfish farms. *Marine Pollution Bulletin* 91. Elsevier Ltd: 185–190. doi:10.1016/j.marpolbul.2014.12.006.

Rose, JM, JG Ferreira, K Stephenson, SB Bricker, M Tedesco, and GH Wikfors. 2012. Comment on Stadmark and Conley (2011) “Mussel farming as a nutrient reduction measure in the Baltic Sea: consideration of nutrient biogeochemical cycles”. *Marine pollution bulletin* 64: 449–51; author reply 455–6. doi:10.1016/j.marpolbul.2011.11.024.

Rumrill, SS, and VK Poulton. 2004. *Ecological role and potential impacts of molluscan shellfish culture in the estuarine environment of Humboldt Bay, Ca. Oregon Department of State Lands, Final Annual Report to the Western Regional Aquaculture Center.*

Schulte, DM, RP Burke, and RN Lipcius. 2009. Unprecedented restoration of a native oyster metapopulation. *Science (New York, N.Y.)* 325: 1124–8. doi:10.1126/science.1176516.

Seitzinger, SP. 1988. Denitrification in freshwater and coastal marine ecosystems: ecological and geochemical significance. *Limnology and Oceanography* 33. Wiley Online Library: 702–724.

Smyth, AR, MF Piehler, and JH Grabowski. 2015. Habitat context influences nitrogen removal by restored oyster reefs. *Journal of Applied Ecology* 52. Wiley Online Library: 716–725.

Smyth, AR, SP Thompson, KN Siporin, WS Gardner, MJ McCarthy, and MF Piehler. 2013. Assessing Nitrogen Dynamics Throughout the Estuarine Landscape. *Estuaries and Coasts* 36: 44–55. doi:10.1007/s12237-012-9554-3.

Song, B, JA Lisa, and CR Tobias. 2014. Linking DNRA community structure and activity in a shallow lagoonal estuarine system. *Frontiers in microbiology* 5. Frontiers Media SA.

STAC. 2013. *Evaluation of the Use of Shellfish as a Method of Nutrient Reduction in the Chesapeake Bay. Chesapeake Bay Program Scientific and Technical Advisory Committee.*

Stadmark, J, and D Conley. 2012. Response to Rose et al. and Petersen et al. *Marine Pollution Bulletin* 64. Elsevier Ltd: 455–456. doi:10.1016/j.marpolbul.2011.12.001.

Stadmark, J, and DJ Conley. 2011. Mussel farming as a nutrient reduction measure in the Baltic Sea: Consideration of nutrient biogeochemical cycles. *Marine Pollution Bulletin* 62. Elsevier Ltd: 1385–1388. doi:10.1016/j.marpolbul.2011.05.001.

Steingruber, SM, J Friedrich, R Gachter, and B Wehrli. 2001. Measurement of denitrification in sediments with the 15N isotope pairing technique. *Applied and environmental microbiology* 67: 3771–3778. doi:10.1128/AEM.67.9.3771.

Thamdrup, B, and T Dalsgaard. 2002. Production of N 2 through Anaerobic Ammonium Oxidation Coupled to Nitrate Reduction in Marine Sediments Production of N 2 through Anaerobic Ammonium Oxidation Coupled to Nitrate Reduction in Marine Sediments. *Applied and environmental microbiology* 68: 1312–1318. doi:10.1128/AEM.68.3.1312.

Tiedje, JM, AJ Sexstone, DD Myrold, and JA Robinson. 1983. Denitrification: ecological niches, competition and survival. *Antonie van Leeuwenhoek* 48. Springer: 569–583.

Underwood, GJC, and J Kromkamp. 1999. Primary Production by Phytoplankton and Microphytobenthos in Estuaries. In *Estuaries: Advances in Ecological Research 29*, 93–153.

Wilson, PS, and K Vopel. 2015. Assessing the Sulfide Footprint of Mussel Farms with Sediment Profile Imagery: A New Zealand Trial. *PloS one* 10. Public Library of Science: e0129894.

Yin, G, L Hou, M Liu, Z Liu, and WS Gardner. 2014. A Novel Membrane Inlet Mass Spectrometer Method to Measure 15 NH 4+ for Isotope-Enrichment Experiments in Aquatic Ecosystems. *Environmental Science & Technology* 48: 9555–9562.

Table 1. Ambient water quality parameters

	Sampling date					
	July	**August**	**October**	**January**	**April**	**June**
[NH_4^+] (µM)	2.0	0.5	0.6	*b.d.*	1.3	0.8
[NO_3^-] (µM)	0.6	*b.d.*	*b.d.*	*0.6*	0.8	*b.d.*
[SRP] (µM)	0.4	*b.d.*	0.3	*b.d.*	0.3	0.3
Temperature (°C)	30	26	20	4	15	26
Salinity (ppt)	24	23	27	25	23	25

b.d. indicates below instrument detection (0.36 µM for NH_4^+ and NO_3^-, and 0.16 µM for SRP).

Table 2. Sediment parameters for each site (0-2 cm depth)

	Porosity	Dry bulk density (g/cm3)	Grain size: % silt and clay*	%C	%N	C/N
Bare	0.49 ± 0.01	1.48 ± 0.02	5.6 ± 1.1	0.16 ± 0.04	0.04 ± 0.01	4.6 ± 1.2
Row	0.53 ± 0.02	1.35 ± 0.05	19.8 ± 2.8	0.36 ± 0.05	0.06 ± 0	5.8 ± 0.9
Oyster	0.72 ± 0.04	0.87 ± 0.08	22.8 ± 2.2	1 ± 0.16	0.14 ± 0.02	6.6 ± 0.5

Annual averages, n=11 to 16. *July 2014 only.

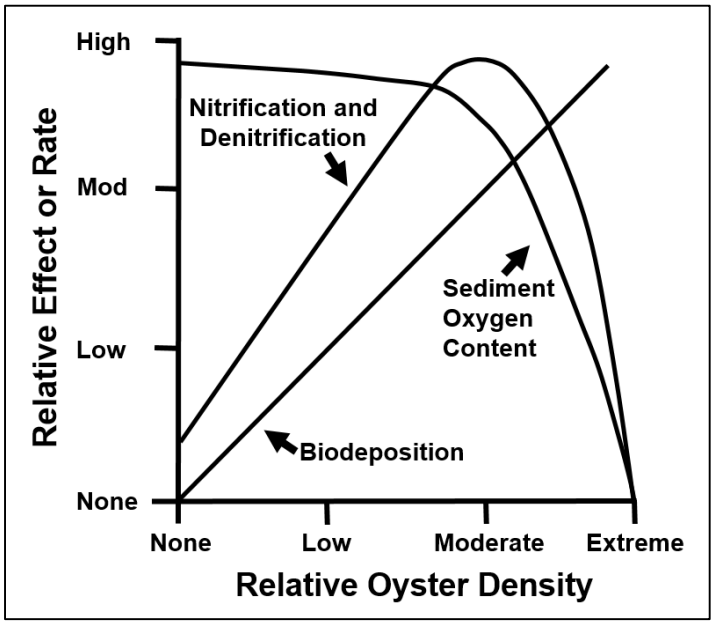

Figure 1. Conceptual model showing the relationship between oyster density and N processes, including sediment denitrification and oxygen demand (Modified from Newell, 2004).

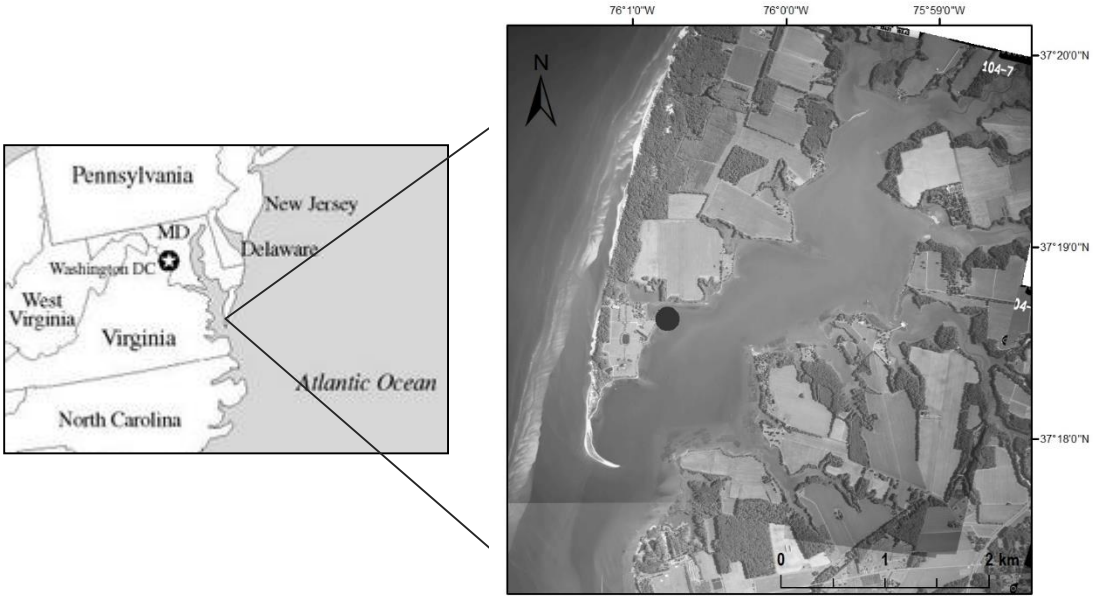

Figure 2. Farm location in Cherrystone Inlet, a tributary of Chesapeake Bay (farm indicated by black circle). Aerial photo shows Cherrystone Inlet in the center, and Chesapeake Bay on the left (Virginia Institute of Marine Science, 2012).

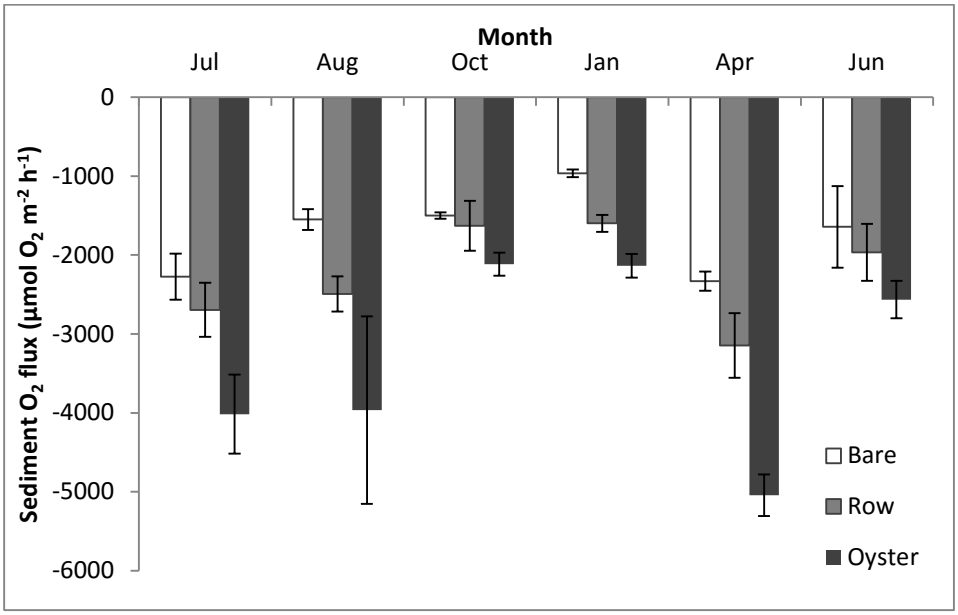

Figure 3. Sediment O_2 flux. Negative values indicate flux directed into sediment. Values are mean of n=3-4 +/- SE.

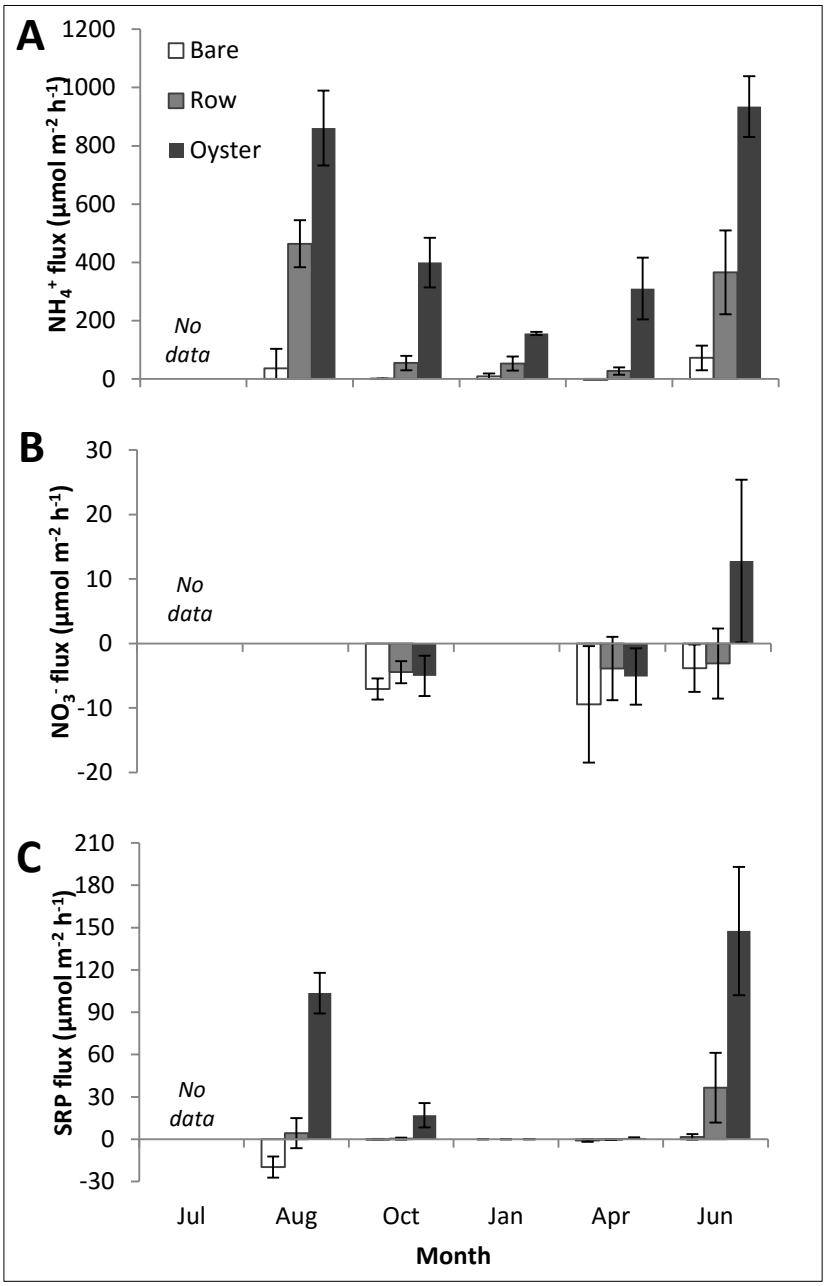

Figure 4. Benthic flux rates of NH_4^+ (A), NO_3^- (B), and SRP (C). Mean +/- SE (n=3-4). Positive and negative values represent fluxes out of and into the sediment, respectively. NO_3^- and SRP fluxes were below detection for August and January, and January, respectively.

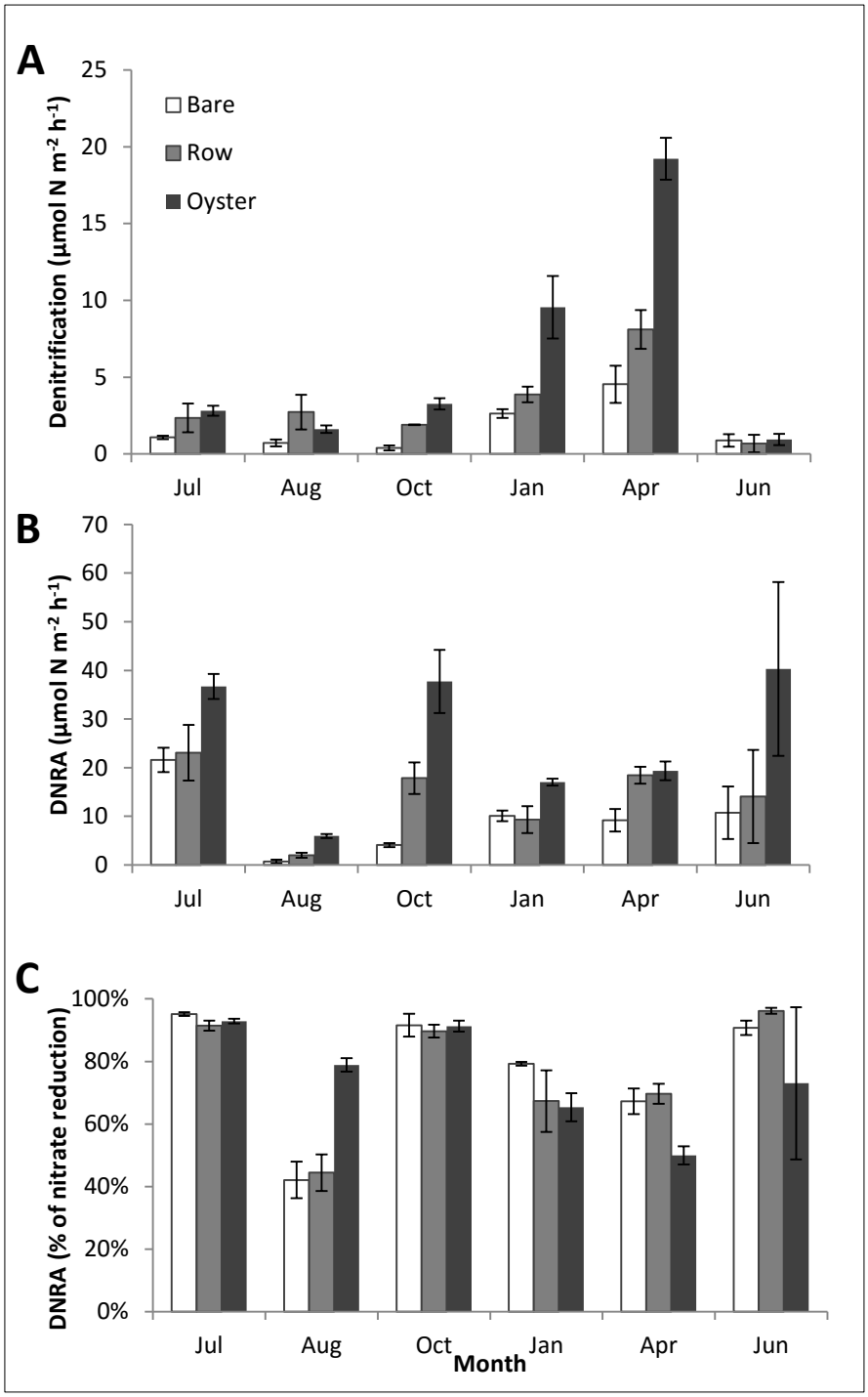

Figure 5. Sediment (A) denitrification rates, (B) DNRA rates, and (C) DNRA as % of NO_3^- reduction. Mean +/- SE (n=3-4, except for Oct Row denitrification, for which n=2).

Appendix to Chapter 1.

Oxygen interference with membrane inlet mass spectrometry may overestimate denitrification rates calculated with the isotope pairing technique*

*To be submitted for publication with the following co-author: Lillian Aoki

Abstract

Membrane inlet mass spectrometer (MIMS) is used to measure gas concentrations in aqueous samples, and specifically is often employed to measure N_2 in denitrification studies. While most denitrification studies using MIMS have employed the N_2:Ar method, MIMS is increasingly used with the isotope pairing technique (IPT), an alternative method that calculates denitrification based on $^{29}N_2$ and $^{30}N_2$ concentrations, measured as the mass to charge ratio (m/z) signals 29 and 30. Dissolved O_2 is known to interfere with m/z 28 and 40 ($^{28}N_2$ and Ar, respectively) in the MIMS, potentially biasing denitrification rates using N_2:Ar. In this study, we show that the O_2 effect on the m/z 29 and 30 signals is also significant, and may result in artificially high denitrification rates with IPT if O_2 varies between samples. In lab-based experiments, m/z 29 and 30 were impacted immediately as O_2 was depleted. The resulting effect on simulated denitrification rates was minor if the final O_2 concentration remained above 50% initial O_2, but increased by more than 100 μmol m^{-2} h^{-1} as O_2 was depleted below 50%. Denitrification rates from sediment core incubations using the IPT technique were an order of magnitude higher when analyzed in the presence of O_2, compared to those analyzed without O_2 using an inline furnace with reduction column. The magnitude of the effect may be machine specific and hence routine calibrations are necessary. Furthermore, the effect is variable over the life of the MIMS. Given these uncertainties, we recommend the use of an inline furnace to remove O_2 for all IPT experiments. Alternatively, the magnitude of the O_2 effect should be assessed often to determine the range of minimal O_2 interference, and all experiments should be conducted within that range.

Introduction

Membrane inlet mass spectrometry (MIMS) is an analytical technique that enables direct, rapid assessment of dissolved gas concentrations in aqueous samples. MIMS is most often used to measure O_2, N_2, and Ar, the three gases with the highest concentrations in aqueous samples at atmospheric equilibrium. The MIMS technique has several advantages over alternative analytical approaches, including high precision of replicate samples and rapid analysis of small sample volumes (Kana et al. 1994). MIMS is commonly used in aquatic sciences, often for study of denitrification.

Denitrification is a microbial process that converts reactive nitrogen to inert dinitrogen gas (N_2) and is an important pathway in the nitrogen cycle at local and global scales (Seitzinger et al., 2006). A common technique used to measure denitrification is the N_2:Ar method, which assesses changes in N_2 concentrations based on the ratio of N_2:Ar. Unlike N_2, Ar is not affected by biological processes, so changes in Ar concentration reflect only physical processes. Therefore, measuring the N_2:Ar ratio minimizes changes in N_2 concentration caused by physical factors and isolates biologically-driven changes. The N_2:Ar ratio also enables clear resolution of small changes in N_2 against high background levels. MIMS has been used in conjunction with the N_2:Ar technique to measure denitrification in a wide variety of systems, including wetlands, aquifers, rice paddies, and streams (Elsey-Quirk et al., 2013; Heffernan et al., 2012; Li et al., 2014; Smith et al., 2006; Whalen et al., 2008)

An alternative approach to measuring denitrification is the isotope pairing technique (IPT). The IPT calculates in situ denitrification rates from the ratio of $^{29}N_2$ and $^{30}N_2$ produced as a result of $^{15}NO_3^-$ amendment (Nielsen, 1992). Low background levels of $^{29}N_2$ and $^{30}N_2$ enable clear detection of denitrification activity. Thus, assuming certain experimental parameters are met, IPT can yield robust denitrification measurements, especially for rates below the detection limit of the N_2:Ar technique (Eyre et al., 2002). For many IPT studies, the $^{29}N_2$ and $^{30}N_2$ isotopes have been measured with an isotope ratio mass spectrometer (IRMS) (e.g. Risgaard-Petersen and Ottosen, 2000; Welsh et al. 2000). However,

some IPT studies now use MIMS to measure $^{29}N_2$ and $^{30}N_2$ (e.g., An and Gardner 2002; Giblin et al. 2010; Hoellein et al., 2014; Bernard et al., 2015; McCarthy et al., 2015).

A consideration in measuring denitrification either by N_2:Ar or IPT methods is that MIMS can be sensitive to variable O_2 concentrations. This effect has been well documented for N_2:Ar applications (Eyre et al., 2004, 2002; Kana and Weiss, 2004). O_2 can interfere with the signals of other gases within the MIMS ion source, potentially impacting their measured concentrations. For the N_2:Ar technique, both the mass to charge ratio (m/z) signals 28 and 40 can be sensitive to this issue. The exact mechanisms for this O_2 effect remain poorly defined and appear to vary between instruments, but two factors seem to be important: 1) O_2 can combine with N_2 in the mass spectrometer ion source to produce NO^+, so with decreasing O_2, m/z 28 ($^{28}N_2$) is effectively increased and m/z 30 (NO^+ and $^{30}N_2$) is decreased (Jensen et al., 1996) ; and 2) variable O_2 concentrations may result in nonlinear ionization efficiencies of the other gases (Emerson et al., 1999). Linearity is a fundamental assumption of MIMS analysis, so O_2-induced non-linearity can cause a detectable effect.

In applications with constant O_2, these effects would be constant, and thus would not bias interpretation of the other signals. However, in applications in which O_2 varies between samples, the magnitude of the effects may vary, potentially introducing analytical error. For example, in denitrification studies, sediment cores are commonly incubated in dark conditions, leading to a decrease in water column O_2. The decreased O_2 concentration between initial and final samples could result in a net positive impact on the m/z 28 signal, erroneously suggesting $^{28}N_2$ production during the incubation. If this 28 signal is used directly, the O_2 effect can lead to overestimated denitrification rates. However, the N_2:Ar technique uses the ratio of 28:40, rather than the 28 signal directly. The 40 signal may be affected by varying O_2 concentrations by the same magnitude as the 28 signal within certain O_2 ranges (Kana and Weiss, 2004). Thus the O_2 effect on the 28:40 ratio (i.e., N_2:Ar) may be negligible if samples remain within the defined O_2 range.

The magnitude and range of the O_2 effect is believed to vary between instruments, so it is critical to verify the machine-specific effect for the range of O_2 concentrations to be analyzed (Eyre et al., 2004). When the O_2 effect is significant, it is not possible to use correction curves to account for the impact of O_2 on the other signals (Eyre et al., 2002). Instead, many experimenters eliminate the O_2 effect by removing O_2 from samples with a copper reduction column heated to 600° C with an inline furnace. This furnace approach is widely used with the N_2:Ar technique to reduce analytical error introduced by the O_2 effect.

In contrast to the N_2:Ar technique, which uses the ratio of two signals, IPT uses the 29 and 30 signals directly. The O_2 effect therefore may be more consequential for calculated denitrification rates. However, the magnitude of the O_2 effect on m/z 29 and 30, and on derived IPT values, has not yet been documented. In this study, we assessed the O_2 effect on m/z 29 and 30 at a range of O_2 concentrations and calculated the subsequent impact of this effect on denitrification rates determined by IPT.

Methods

We conducted laboratory experiments to assess the O_2 impact on m/z 28, 29, 30, and 40 signals measured with the MIMS technique. These signals correspond primarily to $^{28}N_2$, $^{29}N_2$, $^{30}N_2$, and Ar respectively. Following standard MIMS procedures (Kana et al., 1994), dissolved gases were extracted from water samples using a membrane inlet (Bay Instruments) and passed through a cryotrap to remove water vapor and carbon dioxide. Gases were detected with a quadrupole mass spectrometer with a Channeltron secondary electron multiplier (Pfeiffer Balzers Prisma QMS 200).

At the start of each O_2-depletion experiment, a water sample in equilibrium with the atmosphere was sampled and the initial 28, 29, 30, and 40 signals were assessed. O_2 was then slowly depleted from the sample over the course of approximately 30 minutes by step-wise addition of a sodium dithionite ($Na_2S_2O_4$) solution. As O_2 was depleted, the 28, 29, 30, and 40 signals were monitored

to assess their change from the initial conditions. These signals are reported as % of their initial value at 100% O_2 saturation. The water sample was maintained in a temperature-controlled water bath throughout the experiment. Tests were performed at multiple temperatures, from 20 to 30 °C, and at multiple salinities, from 0 to 32 ppt. We also conducted tests prior to and following a standard maintenance replacement of the ion source, which had been used intermittently for six years ("old ion source" and "new ion source" respectively).

The impact of m/z 29 and 30 variation on denitrification rates calculated with IPT equations was then assessed with simulated sediment core incubations across a range of O_2 variation. We used the concentrations of $^{29}N_2$ and $^{30}N_2$ at atmospheric equilibrium as the initial (T_0) concentrations. O_2 was assumed to decrease over the course of the incubation, leading to a change in 29 and 30 signals. The end of incubation concentrations (T_f) of $^{29}N_2$ and $^{30}N_2$ were calculated by adjusting the T_0 (i.e., equilibrium) concentrations by the % change in the 29 and 30 signals observed in the O_2-depletion experiment, per Equation 1.

$$[x]_{Tf([O_2])} = [x]_{equilibium} * \%O_2effect_{([O_2])} \quad (1)$$

where $[x]_{Tf([O2])}$ is the calculated concentration of $^{29}N_2$ or $^{30}N_2$ at the end of the simulated incubation, given a final O_2 concentration; $[x]_{equilibrium}$ is the concentration of that species at atmospheric equilibrium; and $\%O_2effect_{([O2])}$ is the observed effect on the respective signal at the given T_f O_2 concentration. T_f values were calculated in this way for the range of O_2 concentrations assessed during the O_2-depletion tests.

In standard IPT incubations, the changes in 29 and 30 concentrations between T_0 and T_f are used to calculate the in situ denitrification rate, D14 (Nielsen, 1992). In our simulated incubations, the changes in 29 and 30 concentrations due to the O_2 effect between T_0 and T_f were used in this same way

to calculate an "apparent" denitrification rate. The conditions of the simulated incubations were based on experimental conditions used in our laboratory; specifically, a 4-hour incubation of a 10 cm diameter sediment core, containing 1.3 L of water, at 25 °C and 0 ppt salinity.

We calculated these apparent denitrification rates using data from the O_2-depletion tests conducted with both the old and new ion source. With the new ion source, the 30 signal at depleted O_2 concentrations decreased relative to the signal at saturated O_2. Given the structure of the IPT equations, this reduction in the 30 signal results in highly negative apparent denitrification rates, which is an unrealistic result in a system with denitrification activity. In IPT applications in which denitrification occurs, the 30 signal will be significantly increased. Thus, to assess the impact that would be observed in an actual incubation with denitrification activity, we added a constant "actual" denitrification rate to the calculated apparent rates, per Equation 2.

$$Combined\ [x]_{Tf([O_2])} = [x]_{equilibium} * \%O_2effect_{([O_2])} * \%actual\ increase \quad (2)$$

where *%actual increase* is a constant applied to the 29 and 30 signals at all O_2 levels. Based on the observed rates in our field test, we increased the 29 and 30 T_f values by 10% and 700%, respectively, which was equivalent to a denitrification rate of 21 µmol m^{-2} h^{-1}. T_f values therefore reflect both the apparent O_2 effect and the forced actual increase consistent with experimental observations. By comparing denitrification rates calculated from these "combined" values with the "actual" rates, we were able to quantify the impact of O_2-depletion.

In addition to the laboratory tests, we performed a field test in April 2015, in which we analyzed actual IPT sediment incubation samples on the MIMS both with and without O_2 ("no-furnace" and "furnace" respectively). Detailed field and incubation methods are provided in (Lunstrum et al, in preparation). In brief, 9 sediment cores (10 cm ID, 30 cm tall, containing ~12 cm of sediment) were

collected from an oyster (*Crassostrea virginica*) farm in a tributary of Chesapeake Bay. Triplicate cores were taken for each of three sites: two distinct locations within the farm, and a nearby control site. The cores were amended with ~30 µmol $^{15}NO_3^-$, and incubated for 8 hours. Samples were collected from the water column at the beginning of the incubation, and from a slurry of the sediment and the water column at the end of the incubation, according to standard IPT incubation methods (Steingruber et al., 2001). To assess the impact of O_2 depletion on the 29 and 30 signals, duplicate samples from each core were analyzed on the MIMS both with and without an inline furnace (600 °C) and copper reduction column. The furnace and copper column removed O_2 from the gas analyte before it entered the mass spectrometer. Denitrification rates for both the furnace and no-furnace data sets were calculated using standard IPT equations (Nielsen, 1992). Results were compared statistically with ANOVA, assuming normality and assuring homogeneity of variances, log-transforming if necessary.

Results

Changes in O_2 concentration had a significant effect on the other signals during all O_2 depletion experiments. In the new ion source tests, the 28, 29, and 40 signals were impacted similarly, gradually falling to about 98.5% of initial values as O_2 decreased to 70%, and then increasing to 125% of initial values as O_2 approached 0% (Figure 1). The 30 signal had a different pattern, falling to 89% of the initial value at 30% O_2, and then returning to 98% of the initial value as O_2 approached 0%. Given the similar effect on the 28 and 40 signals, the 28/40 ratio (i.e. N_2:Ar) was relatively stable, with a small increase below 50% O_2, ultimately approaching 101% of the initial ratio as O_2 approached 0%.

Repeated O_2 depletion tests on multiple days produced similar results, although the magnitude of the effect varied slightly between independent runs. Additional tests at different temperatures (20, 25, and 30 °C) and salinities (0, 20, and 33 ppt) were also similar, with no apparent temperature or

salinity effect when tested during the same analytical run (data not shown). Figures presented here are therefore representative of the observed patterns, but the exact magnitudes varied slightly day to day.

The results of the old ion source tests (Figure 2) differed in magnitude compared to the new ion source tests (Figure 1). In the old ion source tests, the 28, 29, and 40 signals fell slightly (<1%) and then rose nearly continuously to 150% of initial values as O_2 was depleted. The 30 signal fell slightly more, to a low of 97% of the initial value at 90% O_2, and then rose to 115% as O_2 approached 0%. Although the magnitude of the effects differed before and after the ion source replacement, all tests were similar in that the 28, 29, and 40 signal effects were more positive relative to the 30 signal, a pattern which results in overestimation of denitrification calculated by IPT equations (discussed below).

In the simulated incubations, using the O_2-depletion data alone for T_f values resulted in negative apparent denitrification rates (Figure 3A). After adding an actual rate of 21 µmol m^{-2} hr^{-1}, the "combined" denitrification rate (i.e., the "apparent" rate caused by the O_2 effect plus the "actual" rate) was positive. For the new ion source, the combined denitrification rate showed that the O_2 effect was relatively minor for O_2>50% (Figure 3B). Within this range, the maximum difference between the actual rate of 21 µmol m^{-2} hr^{-1} and the impacted rate occurred at 70% O_2, at which point the combined rate was 18 µmol m^{-2} h^{-1}. Below 50% O_2 concentration however, the impacted denitrification rates rose quickly and exceeded 100 µmol m^{-2} h^{-1} as O_2 was fully depleted. We tested a range of alternative actual denitrification rates, and their associated 29 and 30 values, and the O_2 effect consistently added an apparent denitrification rate of at least 100 µmol m^{-2} h^{-1} as O_2 was depleted.

Compared to the new ion source data, the old ion source data caused an even greater impact on the calculated denitrification rates. Applying the same actual denitrification rate and corresponding 29 and 30 signals for both data sets, the old ion source data showed an impact due to O_2 depletion at 95% O_2, compared to 50% O_2 for the new ion source data (Figure 4). The effect of total O_2 depletion was also

much greater with the old ion source data, with calculated denitrification exceeding 700 µmol m^{-2} hr^{-1} as O_2 approached zero.

In the field experiment, denitrification rates calculated using an in-line furnace (i.e., with O_2 removed from samples) were 5 µmol m^{-2} h^{-1} for the control site, and 8 and 19 µmol m^{-2} h^{-1} for the two oyster farm sites (Figure 5). Variation between replicates was small and the three treatments were significantly different (ANOVA, $p<0.001$). Denitrification rates calculated from the no-furnace data were 29 µmol m^{-2} h^{-1} at the control site and 63 and 112 µmol m^{-2} h^{-1} at the farm site. These rates were significantly higher than the furnace data set for all treatments (ANOVA, $p<0.019$). Samples analyzed without the furnace had greater variability between treatment replicates, but treatments were still significantly different from each other ($p<0.001$).

Discussion

Our results highlight the importance of accounting for the O_2 effect when using IPT equations with MIMS analysis. Both our laboratory tests and field experiment indicated that changes in O_2 concentration alter the 29 and 30 signals. The O_2 effect on the 29 signal was consistently more positive than the effect on the 30 signal, which caused overestimations of denitrification rates in both the simulated incubations and the field experiment.

The pattern of the O_2 effect on the 29 and 30 signals was consistent across all tests; however, the magnitude of the O_2 effect varied between different analytical runs. The reason for this variation is not known, but could be related to subtle differences in analytical run conditions, including for example pumping speed, inlet tubing tension, room temperature, or barometric pressure. The magnitude of the O_2 effect was also inconsistent over the lifetime of the machine. Tests conducted before and after standard maintenance and replacement of the ion source showed notably different results. While the new ion source yielded a zone of minimal O_2 effect for $[O_2] > 50\%$, the old ion source had a smaller zone

of tolerance, and calculated denitrification rates were enhanced at all [O_2] < 95%. Previous work has shown that the O_2 effect on the 28 and 40 signals is machine-specific, and that a given signal may either increase or decrease with decreasing O_2 on different machines (Eyre et al. 2004). Our analysis suggests that the effect is not only machine-specific but also varies slightly between days and considerably over the lifetime of components within the machine.

The standard explanation for variation in the 28 signal with changes in O_2 concentration is that O_2 and N_2 ionize to form NO^+. This reaction effectively decreases the 28 signal (N_2) and increases the 30 signal (NO^+) as O_2 concentration increases. This mechanism is often used to explain signal variation and/or justify corrections (e.g., An and Gardner, 2002; Hoellein et al., 2014; McCarthy et al., 2015). However, the patterns observed in our tests indicate that this explanation is not comprehensive. In all cases, the 30 signal did increase linearly with 28*32, suggesting formation of NO^+ (Jensen et al., 1996), but only within limited O_2 ranges. In the new ion source tests, there was a positive linear relationship between the 30 signal and 28*32 for O_2 concentration greater than 40 to 50%. Below that point, however, there was either little change in the 30 signal, or the relationship reversed and 30 became negatively correlated with 28*32 (Figure 6). In the old ion source tests, this negative relationship predominated at O_2 levels <80% (data not shown). The negative relationship may be caused by higher ionization efficiency at lower O_2 concentrations due to reduced gas pressure (Emerson et al., 1999). We did not attempt to fully explain or determine the mechanisms behind the O_2-dependent signal variation; rather, our aim in this study was to indicate the relationship is more complicated than NO^+ production by O_2 and N_2.

Regardless of the exact mechanism, it is clear that the O_2 effect can alter denitrification rates measured by IPT. The most straightforward way to account for this effect is to use a furnace and copper reduction column to remove O_2 from the samples, thus eliminating O_2 interference. If O_2 removal with an inline furnace is not an option, it may be possible to avoid a significant impact through careful

experimentation and maintaining O_2 concentrations within the zone of minimum interference. For example, in our simulated incubations using the new ion source, there was little alteration of the calculated denitrification rate if the O_2 concentration remained above 50%. This result suggests that with the new ion source, IPT equations could be combined with MIMS analysis without a furnace in experimental situations in which the O_2 concentration remains above 50%. Such conditions could be achieved in flow-through incubations, with short incubation durations, and/or with slurries of relatively oxic sediments. However, the zone of minimal O_2 interference will vary by machine. Furthermore, given the variation we observed between test days and over time, the zone of minimal O_2 effect could change, and should be confirmed with an O_2 test on each day of sample analysis.

Our field study highlights the challenges of avoiding the O_2 effect through experimental procedures. The field study corroborated the O_2 depletion tests' finding that lower O_2 in T_f samples results in artificially enhanced denitrification rates. Assuming the furnace data set (O_2-free) is correct, the no-furnace data set overestimated denitrification by 25 µmol m^{-2} h^{-1} for the control, and 50 to 100 µmol m^{-2} h^{-1} for the farm sites. The T_f field samples were all depleted in O_2 relative to T_0, ranging from 37% saturation for the control, to 22% and 5% for sites #1 and #2, respectively. The very low O_2 levels were the result of geochemical oxidation of highly reduced sediments during slurrying, which stripped O_2 from the slurry mixture. O_2 probes placed in the cores during slurrying showed O_2 concentrations falling from over 50% just after the cores were opened to near 0% in some cores during slurrying. Maintaining an O_2 concentration above 50% in the T_f slurry samples would be difficult if not impossible for the anoxic sediments studied in this experiment.

We attempted to use the O_2-depletion curves and the T_f O_2 concentrations to correct the 29 and 30 signals from the no-furnace data set to match the furnace data set. However, the corrected values still overestimated denitrification and did not correlate well with the furnace rates. We do not try to explain this discrepancy, but rely on the assumption that the furnace data set reflects more accurate

rates and conclude that for our instrument, corrections cannot be made to datasets affected by the O_2 effect.

It is clear from our analysis that O_2 variability has a significant effect on the 29 and 30 signals measured with MIMS. For any application in which individual (i.e., non-ratio) signals are used, as in the IPT, and in which O_2 varies between samples, we recommend removing O_2 from samples during analysis with an inline furnace. If O_2 removal with an inline furnace is not possible, it is imperative to verify that the O_2 effect is negligible over the possible O_2 range of interest. Furthermore, as the effect can vary between days and over the lifetime of an individual machine, the O_2 effect should be assessed often.

Acknowledgements

This research was supported by grants from the National Science Foundation (Virginia Coast Reserve Long Term Ecological Research grant, DEB-1237733), Virginia Sea Grant's Graduate Student Fellowship program, and a student grant from the Virginia Water Resources Research Center. The authors would like to thank Michael Pace and Karen McGlathery at University of Virginia for providing feedback, support, and lab materials. We also thank Todd Kana at University of Maryland Center for Environmental Science Horn Point Laboratory for his advice and technical advice on the MIMS.

References

An, S., Gardner, W., 2002. Dissimilatory nitrate reduction to ammonium (DNRA) as a nitrogen link, versus denitrification as a sink in a shallow estuary (Laguna Madre/Baffin Bay, Texas). Marine Ecology Progress Series 237, 41–50.

Bernard, R.J., Mortazavi, B., Kleinhuizen, A.A., 2015. Dissimilatory nitrate reduction to ammonium (DNRA) seasonally dominates NO3 − reduction pathways in an anthropogenically impacted sub-tropical coastal lagoon. Biogeochemistry 125, 47–64.

Elsey-Quirk, T., Smyth, A., Piehler, M., Mead, J. V, Velinsky, D.J., 2013. Exchange of Nitrogen through an Urban Tidal Freshwater Wetland in Philadelphia, Pennsylvania. Journal of environmental quality 42, 584–595.

Emerson, S., Stump, C., Wilbur, D., Quay, P., 1999. Accurate measurement of O2, N2, and Ar gases in water and the solubility of N2. Marine Chemistry 64, 337–347.

Eyre, B., Rysgaard, S., Dalsgaard, T., Christensen, P., 2002. Comparison of isotope pairing and N2: Ar methods for measuring sediment denitrification—Assumption, modifications, and implications. Estuaries 25, 1077–1087.

Eyre, B., Rysgaard, S., Dalsgaard, T., Christensen, P., 2004. Reply to Comment on Our Paper "Comparison of Isotope Pairing and N2:Ar Methods for Measuring Sediment Denitrification". Estuaries 27, 177–178.

Heffernan, J.B., Albertin, A.R., Fork, M.L., Katz, B.G., Cohen, M.J., 2012. Denitrification and inference of nitrogen sources in the karstic Floridan Aquifer. Biogeosciences 9, 1671–1690.

Hoellein, T.J., Zarnoch, C.B., Grizzle, R.E., 2014. Eastern oyster (Crassostrea virginica) filtration, biodeposition, and sediment nitrogen cycling at two oyster reefs with contrasting water quality in Great Bay Estuary (New Hampshire, USA). Biogeochemistry 122, 113–129.

Jensen, K.M., Jensen, M.H., Cox, R.P., 1996. Membrane inlet mass spectrometric analysis of N-isotope labelling for aquatic denitrification studies. FEMS Microbiology Ecology 20, 101–109.

Kana, T., Weiss, D., 2004. Comment on "Comparison of isotope pairing and N2:Ar methods for measuring sediment denitrification" by BD Eyre, S. Rysgaard, T. Dalsgaard, and P. Bondo Christensen. 2002. Estuaries 25: 1077–1087. Estuaries and Coasts 27, 173–176.

Li, X., Xia, L., Yan, X., 2014. Application of membrane inlet mass spectrometry to directly quantify denitrification in flooded rice paddy soil. Biology and fertility of soils 50, 891–900.

McCarthy, M.J., Newell, S.E., Carini, S. a., Gardner, W.S., 2015. Denitrification Dominates Sediment Nitrogen Removal and Is Enhanced by Bottom-Water Hypoxia in the Northern Gulf of Mexico. Estuaries and Coasts 1–16.

Nielsen, L.P., 1992. Denitrification in sediment determined from nitrogen isotope pairing. FEMS Microbiology Letters 86, 357–362.

Seitzinger, S., Harrison, J.A., Böhlke, J.K., Bouwman, A.F., Lowrance, R., Peterson, B., Tobias, C., Drecht, G. Van, 2006. Denitrification across landscapes and waterscapes: a synthesis. Ecological Applications 16, 2064–2090.

Smith, L.K., Voytek, M.A., Böhlke, J.K., Harvey, J.W., 2006. Denitrification in nitrate-rich streams: Application of N2: Ar and 15N-tracer methods in intact cores. Ecological Applications 16, 2191–2207.

Steingruber, S., Friedrich, J., Gachter, R., Wehrli, B., 2001. Measurement of denitrification in sediments with the 15N isotope pairing technique. Applied and environmental microbiology 67, 3771–3778.

Whalen, S.C., Alperin, M.J., Nie, Y., Fischer, E.N., 2008. Denitrification in the mainstem Neuse River and tributaries, USA. Fundamental and Applied Limnology/Archiv für Hydrobiologie 171, 249–261.

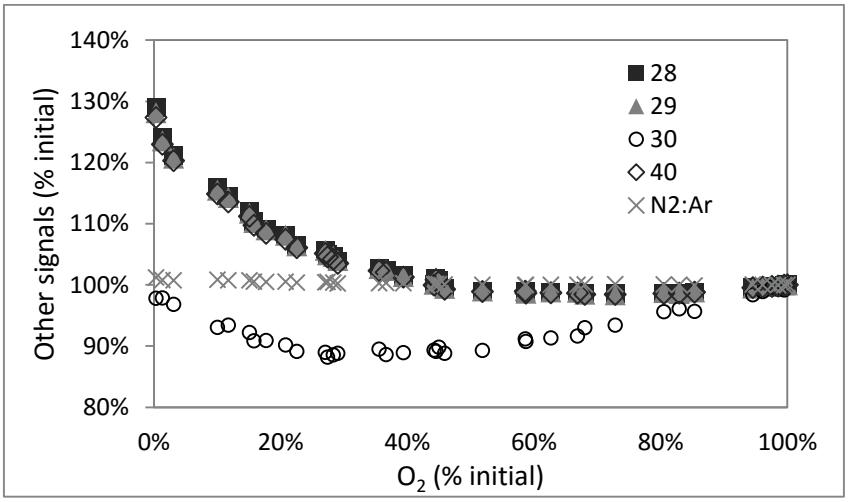

Figure 1. O_2 effect on other signals with the new ion source (25° C, 0 ppt)

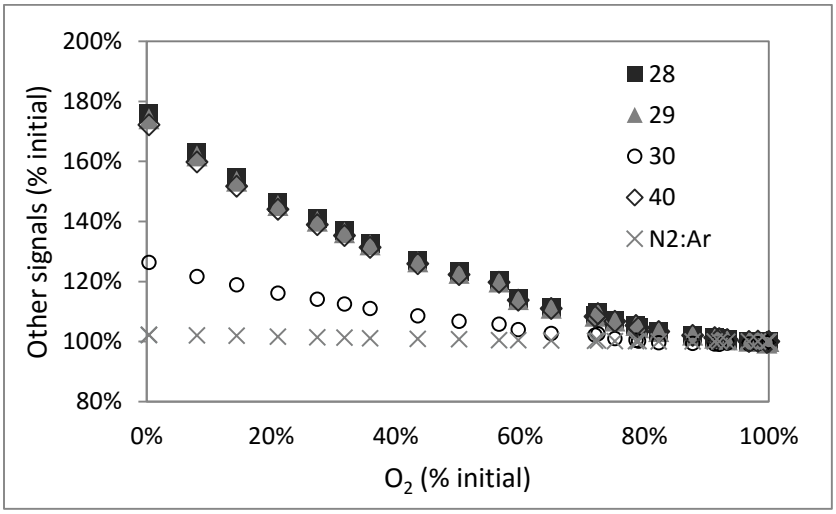

Figure 2. O_2 effect on other signals with the old ion source (25° C, 0 ppt)

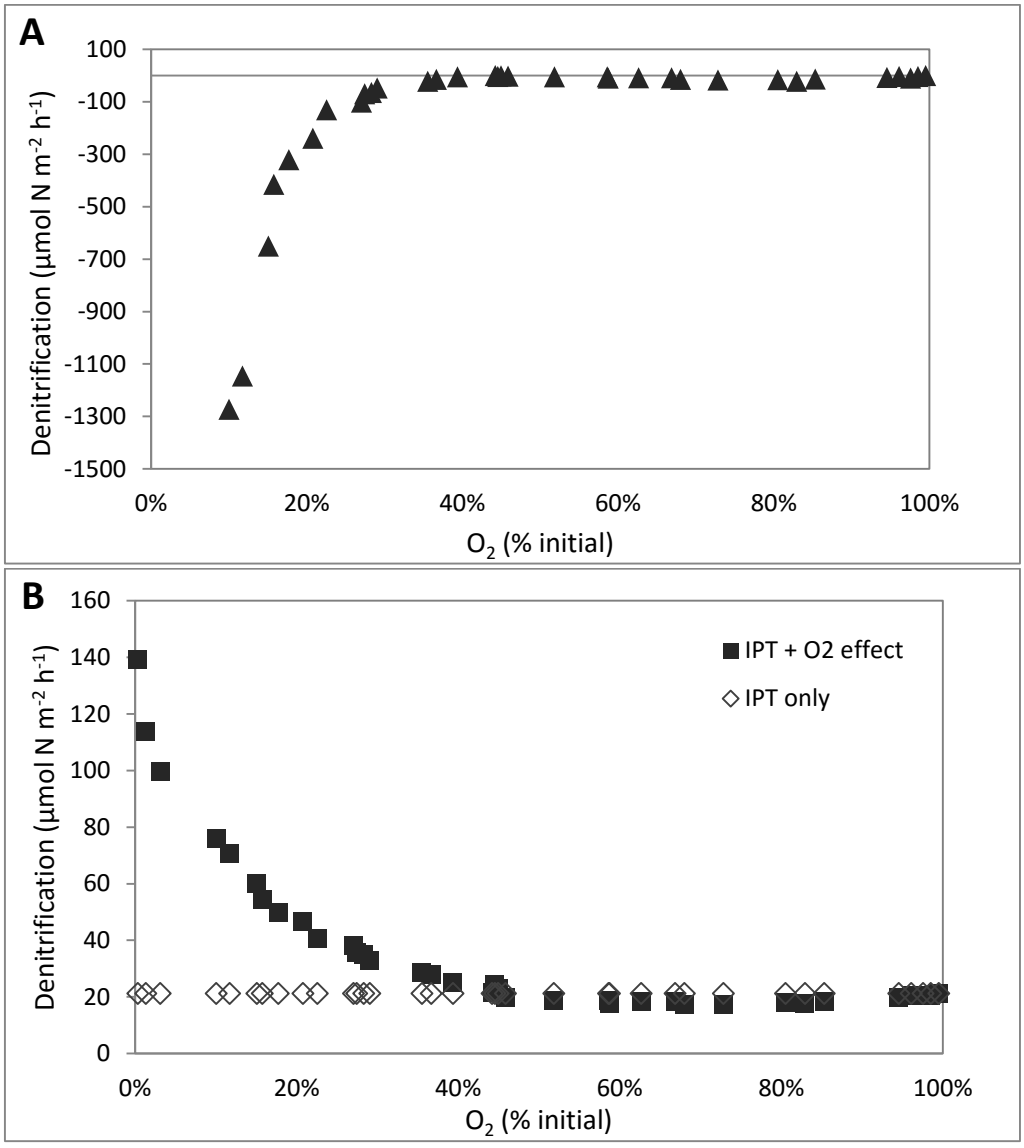

Figure 3. Effect of variable O_2 on denitrification rates, in isolation (A) and in addition to a small "actual" denitrification rate (B). In B, diamonds represent the actual rate (21 µmol N m^{-2} h^{-1}), and squares represent the combined rate (actual rate plus O_2 effect). Calculations use data from the new ion source tests.

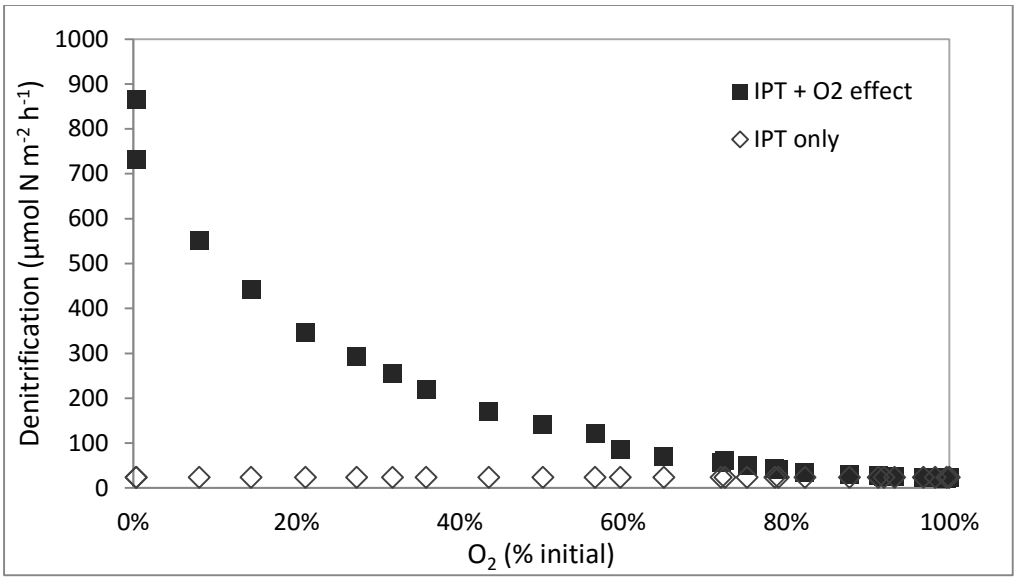

Figure 4. Effect of variable O_2 on denitrification rates using data from the old ion source tests. Diamonds represent the "actual" rate (21 µmol N m^{-2} h^{-1}), and squares represent the combined rate (actual rate and O_2 effect).

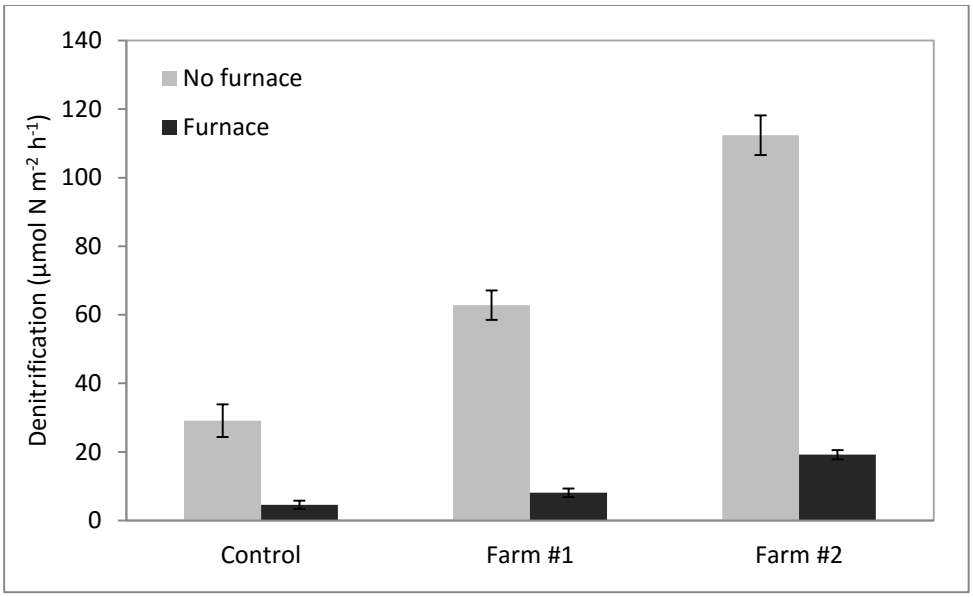

Figure 5. Denitrification with and without inline furnace for the sediment core incubations. Mean +/- SE (n=3 to 4).

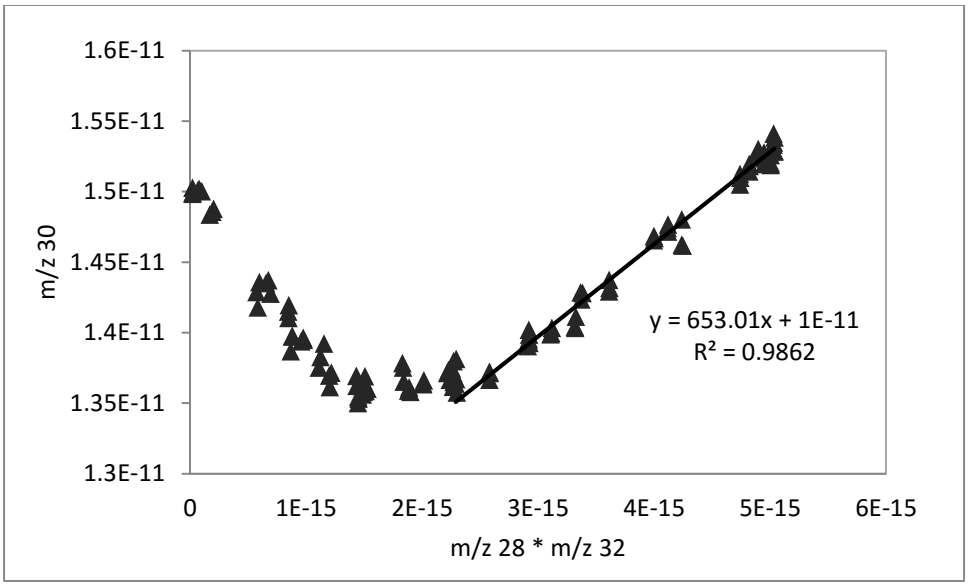

Figure 6. Relationship between 30 signal and 28*32 signal for decreasing O_2 concentrations.

Chapter 2.

Quantifying nitrogen bioextraction with oyster aquaculture in a tributary of Chesapeake Bay*

*To be submitted for publication with the following intended co-authors: Karen McGlathery, Suzanne Bricker, Mark Brush

Abstract

Bivalve aquaculture has been proposed as a tool to mitigate nutrient pollution in coastal areas where conventional methods alone cannot sufficiently achieve water quality goals. By filtering plankton from the water column, bivalves can potentially sequester nutrients from the aquatic system. Oyster aquaculture in particular is being advocated to reduce nitrogen (N) concentrations in some areas, although limited data has fueled debate about its effectiveness. Disagreement revolves around three main issues: the total N extraction capacity, including through harvest, burial, and denitrification; the balance of these extractive pathways with regenerative processes that return reactive N to the water column; and the extent to which oyster aquaculture can significantly reduce watershed N loads given realistic expansion of the industry. We addressed all three issues by measuring relevant processes at a rack and bag eastern oyster (*Crassostrea virginica*) farm in a tributary of Chesapeake Bay. Total N extraction—including harvest, denitrification, and accumulation in sediment—was 28.8 (±1.2) g N m^{-2} y^{-1}, 69% of which was due to harvest alone. Sediment N accumulation relative to a reference site contributed 30%, and enhanced denitrification accounted for <1% of N removal. Applying this extraction rate to the area currently leased for aquaculture use in the inlet, we estimated that 54,805 (±2,295) kg N y^{-1} could be extracted, accounting for 162% of the watershed N load. However, N regeneration processes were comparable in magnitude to total N extraction, and benthic NH_4^+ flux was 28.2 (±2.0) g N m^{-2} y^{-1}. Although NH_4^+ flux was enhanced, ambient nutrient concentrations remained low and adverse impacts associated with eutrophication were not observed, likely due to regular farm maintenance and tidal flushing. Thus, it appears that oyster aquaculture can be an effective tool to mitigate nutrient loading in this inlet and other water bodies with similar characteristics.

Introduction

Eutrophication is a globally prevalent and persistent phenomenon caused by excessive nutrient loading to coastal waters (Nixon 1995). Enhanced nutrient loading supports high rates of primary productivity, which can lead to a range of adverse ecological problems including nuisance or toxic algae blooms, loss of submerged aquatic vegetation, hypoxic "dead zones", and fish mortality (Cloern 2001). Chesapeake Bay has experienced some of these consequences of eutrophication since at least the 1950s (Kemp et al. 2005), and while billions of dollars have been spent to control nutrient inputs, the Bay remains highly eutrophic (Butt and Brown 2000; S Bricker et al. 2008). Efforts to reduce nitrogen (N) pollution from point sources (e.g., sewage outflow) have been successful in many sectors, but non-point source pollution, for example from agricultural runoff, has been more difficult to control (Boesch et al. 2001). Along with onsite reduction strategies like improved fertilizer management and expanded riparian buffers, alternative strategies that sequester N downstream are being considered to mitigate upstream pollution.

Bivalve aquaculture has been proposed as one such alternative to sequester N pollution. This concept is commonly referred to as "nutrient bioextraction." Bivalves like clams, mussels, and oysters filter particulate matter from the water column and assimilate a portion of the consumed N in their tissues. Because bivalves do not require additional feed inputs, this filtering activity effectively removes plankton-bound N from the water column. The consumed N can be permanently removed from the aquatic system when the bivalves are harvested. However, on average only 30% of the N consumed is assimilated, and the remainder is returned to the environment in either dissolved or solid form (Bouwman et al. 2013). Solid excreted matter, commonly called biodeposits, sinks to the sediment where it may ultimately be remineralized, denitrified or buried. The latter two processes, denitrification and burial, effectively remove reactive N from the water column and can be considered additional extraction pathways.

Oyster aquaculture in particular is being considered for nutrient bioextraction in Chesapeake Bay and other estuaries on the east coast of the US, as historic reefs and associated ecosystem functions have been severely diminished (NOAA 2011; Newell and Mann 2012; STAC 2013). Modeled data indicate that oyster-mediated N extraction may be comparable per unit area to existing water quality management practices for stormwater and agricultural systems (J Rose et al. 2014), and economic analyses have suggested that costs may be lower than such alternatives for Chesapeake Bay (Stephenson et al. 2010). Despite these results, oyster aquaculture has not been approved as a best management practice because its net effect on coastal N is not well understood. Debate is focused on three main issues. First, while the N extracted in harvest is relatively simple to quantify, burial and denitrification remain poorly constrained due to methodological difficulties and limited data. Thus, estimates of total N bioextraction including all three pathways are somewhat speculative. Second, although benthic denitrification and burial contribute to N extraction, biodeposited particulate N can alternatively be mineralized to ammonium (NH_4^+), a reactive form of N that can exacerbate local eutrophication. The balance between this N regeneration and extractive processes needs to be better defined in order to understand the net effect of aquaculture biodeposition on water quality (Stadmark and Conley 2011; JM Rose et al. 2012; Stadmark and Conley 2012; Petersen et al. 2014). Finally, even if the first two issues are clarified, the efficacy of oyster aquaculture to significantly mitigate terrestrial N loading depends on the extent to which it can be expanded in realistic situations (Bricker et al., 2014a; Land, 2014).

Oyster N bioextraction has been studied over the past decade using both models (Ferreira et al. 2009; JM Rose et al. 2015) and field measurements (Grizzle and Ward 2011; Carmichael et al. 2012; Higgins et al. 2013; Sebastiano et al. 2015). However, these studies focus almost exclusively on harvested N, and none have yet provided measurements for harvest, denitrification and burial at an active farm site. When burial and denitrification are considered, rates are typically etrapolated from

laboratory experiments or oyster reefs, not from in situ measurements (Newell et al. 2005; Carmichael et al. 2012). Furthermore, N harvest quantified in field studies is often estimated from short-term assimilation experiments, not actual harvest data incorporating industry practices (Grizzle and Ward 2011; Carmichael et al. 2012; Sebastiano et al. 2015).

This study evaluates oyster aquaculture as a N bioextraction tool by measuring the relevant processes on an active farm. Focusing on a small, near-bottom oyster farm in a tributary of Chesapeake Bay, we measured all three N extraction pathways, including harvest, denitrification, and sediment N accumulation. We used actual harvest data and location-specific measurements to provide rates that are largely indirectly estimated in similar studies. We also measured benthic N regeneration in order to put extraction into a broader context of N cycling. Finally, we extrapolated these values to realistic areas of aquaculture expansion to assess the potential impact on inlet nutrient concentrations.

Methods

Site description

Cherrystone Inlet is a shallow tributary of the lower Chesapeake Bay on the Virginia Eastern Shore, USA (Figure 1). Situated approximately 25 km from the mouth of the Bay, Cherrystone is characterized by relatively high tidal flushing, with a tidal prism of approximately 1/2 the inlet volume per day (Kuschner 2015). Ambient water conditions are influenced by significant marine input, and salinity fluctuates between 17 and 27 ppt (Kuschner 2015). The inlet covers 5.7 km^2, with a mean depth of 1.1 m at mean sea level, and approximately 30% of the sub-tidal area (1.9 km^2) is reserved as private shellfish leases (Kuschner 2015). The leases are primarily utilized for hard clam (*Mercenaria mercenaria*) cultivation, which at the time of this study covered approximately 0.2 km^2, with smaller areas used for eastern oysters (*Crassostrea virginica*) (Emery 2015). The farm in this study cultivates oysters using the "French" rack and bag method, in which oysters are grown in mesh bags (approximately 50 x 90 cm in

this case), on racks approximately 30 cm above the sediment surface. Oyster density ranged from 300 individual oysters per bag for harvest class to 1200 individuals per bag for seed 5 mm to 2.5 cm in diameter. The farm occupied approximately 925 m^{-2}, and consisted of 7 oyster racks, each measuring 46 m by 0.9 m. At the time of this study, the farm had been in operation for approximately four years. Annual seeding was 130,000 oyster seeds, and harvest was approximately 65,000 market-sized oysters per year. On an areal basis, the seeding density was 140 oyster m^{-2}, and harvest density, after the observed 50% mortality rate, was 70 harvested oysters m^{-2}. This density is typical of commercial oyster farms.

Field and laboratory procedures

Annual N extraction via harvest was calculated by combining harvest data with measured oyster N content. N content was assessed from 10 harvest class oysters (as defined by the farmer) in July and October, 2014. Although oysters are harvested year-round by the farmer, we assumed these two seasons to represent the annual average as the oysters vary little in size over the course of the year (personal communication from the farmer). Before analysis, shells were gently rinsed, but were not scrubbed to remove minor algal growth, thus replicating actual harvest conditions. Shell dimensions, total wet weight, and tissue and shell wet weight were recorded for each oyster. Shell and tissue were then dried to constant weight in a 60° C oven and dry weights recorded. Each tissue and shell was then ground with a mortar and pestle, and 5 mg subsamples were analyzed for %N on a Carlo Erba NA 2500 Elemental Analyzer. Total N content per oyster was calculated by multiplying the dry weight of shell and tissue by the respective %N content. The average total N content of the 20 oysters was multiplied by the annual harvest to calculate total N extraction via harvest. Harvest data was provided by the farmer for a 12-month period in 2013-2014. We assumed the annual N input from seed (5-6 mm) to be minimal and did not subtract this from the harvest N value.

Denitrification and benthic NH_4^+ flux were assessed seasonally in 2014 and 2015 using sediment core incubations. Nitrate (NO_3^-) fluxes were also measured, but these were small relative to NH_4^+ flux (typically <±10 μmol N m^{-2} h^{-1}), and are thus not included in this analysis. Detailed methods for these measurements are provided in Chapter 1, but relevant information is summarized here. Incubations were performed in July, August, October, January, April, and June. The October, January, and April incubations were considered representative for fall, winter, and spring, respectively, and data from the July, August and June incubations were pooled for summer values. Measurements were taken at two locations within the farm—directly under oyster racks ("Oyster") and in between racks ("Row")—as well as at an unvegetated reference site 40 m from the farm ("Bare"). To calculate the enhancement of each process in the farm, the average Bare rates were subtracted from the average Row and Oyster sites for each season. The annual enhancement for each farm location was then taken as the average of the seasonal enhancement values. The farm average enhanced denitrification and NH_4^+ fluxes was calculated as the weighted average of the Oyster and Row rates, and their respective surface area in the farm (i.e., the area under the oyster racks, and in between racks for Oyster and Row). We also calculated the denitrification efficiency (DE) for each site as the ratio of denitrification to the sum of denitrification and NH_4^+ flux, ignoring the minor NO_3^- fluxes. DE is a measure of the relative rate of denitrification compared to total benthic N fluxes.

Burial was estimated as sediment N accumulation based on the difference in sediment N content in the farm versus at the Bare site. In May 2015, 8-cm sediment cores were collected with a 2.6-cm ID corer at the Bare, Oyster, and Row sites, as well as at locations on the edge of the Oyster racks (n=6 to 9). The latter samples were taken to assess potential intermediate levels of accumulation in between Oyster and Row sites. To assess total N content and characterize the N profile, the 8-cm cores were sectioned into 0-2 cm, 2-5 cm, and 5-8 cm depths. Each depth section was dried until constant weight at 60° C, and then dry weight measured. Dry bulk density was calculated for each depth section

as the dry weight divided by sample volume. 25 mg subsamples were then analyzed for %N on a Carlo Erba NA 2500 Elemental Analyzer. The total areal N content for the 0-8 cm depth was calculated by multiplying dry bulk density and %N for each depth section, and then summing the N content of the three sections. Replicates from each site were then averaged. Accumulation rates were estimated by subtracting the N content at the Bare site from the Oyster, Row, and edge of Oyster values, and then dividing by the age of the farm (4 years 9 months at the time of the sediment collection). The average annual N accumulation in the farm sediment was calculated in a similar manner as denitrification: the accumulation rates for Row and Oyster were multiplied by the area of the respective surface area, and the weighted average taken as the farm-average accumulation rate. The total N content at the Oyster edge samples was more similar to the Row than Oyster sites for some depths, indicating that the higher accumulation rate in the center of oyster racks may not be representative of the entire sediment area under the racks (Figure 4). Therefore, the average of the Oyster and Edge of Oyster rates was used to calculate the accumulation rate for the area under oyster racks.

N bioextraction calculations

Total N bioextraction for the farm was calculated by summing N extraction via harvest, sediment accumulation and denitrification. To compare this rate to location-specific nutrient loading, total bioextraction was also calculated as a percent of the annual N load into the inlet from atmospheric and terrestrial sources. The annual total N (TN) load to the inlet was estimated by Kuschner et al. (2015) using the Nitrogen Loading Model (NLM), at 33,759 kg N y^{-1}. Normalized for watershed area, this was equal to 0.9 g N m^{-2} watershed y^{-1}. The NLM model was originally developed for Cape Cod (Valiela et al. 1997), but has been adapted for the Delmarva Peninsula, for which most results are within 38% of measurements (Cole 2005, Giordano et al. 2011). The model incorporates N inputs from atmospheric deposition, fertilizer using application rates specific to Virginia, and human waste in septic systems.

Poultry waste can also be incorporated, but there were no poultry farms in Cherrystone Inlet during this study.

Results

Harvested oysters averaged 80.1 mm in length, slightly larger than minimum standard oyster size of 76 mm, with a wet weight of 68.1 g (Table 1). Shell and tissue %N were 0.18% and 7.16%, respectively. Total N content was 0.28 g per oyster, 70% of which was contained in tissue and the remaining 30% in shell. Combined with the annual number of oysters removed by harvest, total bioextraction through harvest was 18,365 (± 543 standard error) g N y^{-1}. Given the farm size of 925 m^{-2}, the areal N harvest was 19.9 (± 0.6) g N m^{-2} y^{-1}.

Denitrification rates were significantly enhanced within the farm relative to the Bare site for all seasons (ANOVA, p<0.006), except summer when rates were very low at all sites (data in Chapter 1) (Figure 2). Despite the enhancement, rates were relatively low for all sites and seasons, with a maximum measured rate of 19.2 (±1.4) µmol N m^{-2} h^{-1} at the Oyster sites in spring. The resulting annual average enhancement was 1.8 (± 0.5) and 6.3 (± 0.7) µmol N m^{-2} h^{-1} at the Row and Oyster sites, respectively. Multiplying these enhancement rates by the respective area of each surface type yielded a farm average denitrification enhancement of 3.2 (± 0.4) µmol N m^{-2} h^{-1}, equivalent to 0.4 (± 0.05) g N m^{-2} y^{-1}. The farm area-integrated total for enhanced denitrification was thus 362.7 (± 45.3) g N y^{-1}.

Enhanced NH_4^+ flux was two orders of magnitude higher than denitrification (Figure 3). NH_4^+ flux from Oyster and Row sites were consistently and significantly higher than the Bare sites, reaching a maximum of 903.2 (±75.5) µmol N m^{-2} h^{-1} under oyster racks in summer (data presented in Chapter 1). The resulting average enhancement for the farm was 229.4 (±16.5) µmol N m^{-2} h^{-1}, equivalent to 28.2 (± 2.0) g N m^{-2} y^{-1}. Multiplied by farm area, total NH_4^+ flux enhancement was thus 26,040 (± 1,868) g N y^{-1}. Because of the relatively high farm NH_4^+ fluxes, DE was lower within the farm for all seasons. At the Bare

site, seasonal DE ranged from 24% to 69%, whereas the farm sites ranged from 0% in summer to 9% and 28% in spring for Row and Oyster, respectively.

Sediment %N was relatively low at all sites, but significantly higher in the farm sites compared to the Bare site for all depth subsections (ANOVA with LSD post-hoc, $p<0.009$). Bare site %N ranged from 0.009% to 0.024%, whereas the farm sites ranged from 0.03% to 0.076% (Figure 4). The 8-cm depth-integrated N content was 13.3 (± 1.7) g N m^{-2} at the Bare site compared to 51.2 (± 7.0) g N m^{-2} at the Row sites, and 60.7 (± 15.3) g N m^{-2} at the Oyster sites. The farm-average accumulation rate calculated from these values and the age of the farm was 8.6 (± 1.1) g N m^{-2} y^{-1}. This value thus represents enhanced N accumulation, in excess of the rate at the Bare site. Integrated over the farm area, this equaled 7,953.3 (± 975.2) g N y^{-1} (Figure 5).

Total N bioextraction considering all three processes was 28.8 (± 1.2) g N m^{-2} y^{-1}, for an annual farm total of 26,681 (± 1,117) g N y^{-1}. Harvest accounted for 69% of the total, followed by enhanced sediment accumulation at 30%, and enhanced denitrification accounting for <1% (Figure 5). Extrapolating the areal bioextraction rates to the total leased area of the inlet (1.9 km^2), 54,805 (±2,295) kg N y^{-1} could be extracted by all three processes, equivalent to 162% of the annual load. Considering harvest alone, 112% of the N load would be removed.

Discussion

N extraction pathways: harvest, sediment accumulation and denitrification

Harvest

The estimated rate of N extraction by oyster harvest varies widely in bioextraction studies, and the rate measured in the present study (19.9 g N m^{-2} y^{-1}) was on the low end of this range. Higgins et al. (2011) calculated harvest rates of 18.9 to 37.8 g N m^{-2} y^{-1}, given a 24-month or 12-month time to harvest, respectively. In one of the highest estimates, Sebastiano et al. (2015) estimated N extraction up

to 133 g N m^{-2} y^{-1} assuming harvest after a single season and high-density cultivation practices. Modeled assimilation values also yield higher rates, typically exceeding 50 g N m^{-2} y^{-1} (Bricker et al., 2014b; Ferreira et al., 2009; Rose et al., 2015). Areal N harvest is a straight-forward multiplication of N content per oyster with harvest density, so differences in N content, as well variation in "harvest density" parameters—e.g., mortality, time to harvest and stocking density—can impact the harvest N extraction rate.

In this study, harvested N was low relative to other bioextraction studies due to relatively low stocking density, longer time to harvest, and high mortality. The seeding density at our farm was 140 oysters m^{-2}, which is typical of commercial oyster farms, although densities over 1000 oysters m^{-2} are reported in some studies (Carmichael et al., 2012; Rose et al., 2015; Don Webster, personal communication). Similarly, a relatively long average time to harvest (18 to 24 months) at our site resulted in a low N harvest rate relative to other studies. In areas with faster time to harvest, or in situations where sub-market sized oysters (which have higher N assimilation rates) are harvested, short-term extraction rates can be significantly higher (Carmichael et al. 2012; Dalrymple and Carmichael 2015; Sebastiano et al. 2015). In the latter case, while measured rates may be reasonable for bioextraction-specific projects, they would exceed extraction rates for commercial aquaculture operations which harvest larger oysters. Finally, while mortality is highly variable, rates lower than the 50% observed at our site, e.g., <20%, have been observed in other studies (Higgins et al. 2011; Sebastiano et al. 2015). When field data are limited, bioextraction studies often assume these harvest density factors based on other data sets, and thus run the risk of inappropriately extrapolating site-specific results. Therefore, it is important for field studies to clearly explain these parameters.

N content per oyster is relatively well constrained, and the value at our site (0.28 g) lies within the range of published values, which can be below 0.2 g (Higgins et al. 2011; Sebastiano et al. 2015) to >0.35 g (Carmichael et al. 2012; Dalrymple and Carmichael 2015). This variation can result in

differences in projected N harvest estimates (e.g., Bricker et al., 2014a; Land, 2014). However, relative to other uncertainties, the variability is small and literature values can reasonably be extrapolated to larger studies. Furthermore, oyster N content is a simple metric to measure, so estimated values can be field-verified with little effort.

Denitrification

Denitrification measurements from oyster farms are not common, so previous bioextraction studies have assumed denitrification rates based on laboratory tests or measurements in oyster reefs (Bricker et al., 2014b; Carmichael et al., 2012; Newell et al., 2005). However, these rates are typically much higher than those observed in our study. For example, based on laboratory results using algae pellets as a proxy for oyster biodeposits, Newell et al (2005) estimated denitrification at 0.5 g N y^{-1} g^{-1} tissue dry weight. Assuming our measured values of 0.28 g tissue dry weight, and density of 70 harvest-sized oysters m^{-2} at our farm, Newell's values would result in denitrification rates of 9.8 g N m^{-2} y^{-1}, which is more than an order of magnitude higher than our measured enhancement of 0.4 g N m^{-2} y^{-1}. Similarly, the high rates found in oyster reefs (Kellogg et al. 2013), equivalent to 57 g N m^{-2} y^{-1}, have also been referenced in bioextraction studies. While our study shows denitrification enhancement within the farm at relatively low rates, the other existing studies of denitrification in oyster aquaculture have not found any significant farm enhancement (Kellogg et al. 2014). Thus, assuming high rates for oyster aquaculture settings may not be appropriate, and may significantly overestimate the contribution of denitrification to N bioextraction.

Absolute rates of denitrification within the farm were also low compared to estuarine rates in general. For example, maximum seasonal denitrification was 19.2 µmol N m^{-2} h^{-1} for Oyster sites in spring, compared to rates up to 83 µmol N m^{-2} h^{-1} at other subtidal locations in Chesapeake Bay and up to 250 µmol N m^{-2} h^{-1} in other estuaries (Cornwell et al. 1999; Kana et al. 2006). The limited

denitrification could have resulted from several potential factors, including low ambient nitrate (NO_3^-), inhibition of coupled nitrification-denitrification caused by anoxic sediment conditions, and dominance of dissimilatory nitrate reduction to ammonium (DNRA) (see Chapter 1). In environments with high ambient NO_3^-, denitrification can be fueled directly from the water column. However, at low NO_3^- sites like ours, NO_3^- must be produced in situ via nitrification, which is inhibited by sediment anoxia (Henriksen and Kemp 1988). At our site, nitrification appeared to be limited by sediment anoxia, as discussed in detail below. Denitrification was further limited by dominance of DNRA as a NO_3^- reduction process. DNRA competes with denitrification by utilizing the same electron acceptor (NO_3^-), and at our site it accounted for an average of 70% of total NO_3^- reduction.

Sediment anoxia and inhibited nitrification-denitrification could have resulted from excessive organic matter (OM) loading within the farm. Conceptual models suggest that denitrification should be enhanced by biodeposition at low to moderate oyster densities, but inhibited at higher densities, as excessive OM loading depletes sediment O_2, inhibiting nitrification-denitrification (Newell 2004). The oyster density at our farm was considered moderate for typical, commercial oyster farms, but denitrification was nonetheless inhibited by anoxic conditions. Sediment anoxia was evident from very high rates of O_2 demand and highly reduced conditions (Chapter 1). Apparently, OM loading even at this "moderate" oyster density exceeded the rate at which sediment O_2 levels and nitrification could be maintained. In more polluted systems where denitrification could be fueled by water column NO_3^-, denitrification could potentially be enhanced at these oyster densities. This phenomenon has been observed in high density mussel farms, where denitrification was significantly higher when ambient NO_3^- levels were seasonally elevated (Nizzoli et al. 2006). However, at our site and others with low ambient NO_3^-, denitrification may be low or inhibited at standard aquaculture densities.

Even though there was slight denitrification enhancement in the farm, it is not clear that this enhancement results in a net increase in denitrification at the landscape level. The lower DE observed

within the farm indicates that a higher proportion of deposited N is remineralized, rather than denitrified, in the farm relative to the Bare site. Considering this trend on the basin scale implies that enhanced deposition within the farm may actually *decrease* landscape-level denitrification (Petersen et al. 2012). Thus, even though N removal by denitrification is locally enhanced, the net impact on basin-scale water quality may be an increase in N regeneration. Given this possibility, as well as the relatively small enhancement observed at our site, and similar data from other studies, benthic denitrification should not be considered an important bioextractive pathway.

It should be noted that this study considered only sediment denitrification, and did not consider possible denitrification occurring on the oysters themselves. Limited data indicate that denitrifying microbes may be active on or in oysters themselves, which would be an additional N bioextraction pathway (Smyth et al. 2013). However, the available measurements are questionable, as the N_2 analysis was conducted on a membrane inlet mass spectrometer (MIMS) without an inline furnace, which can significantly overestimate denitrification due to O_2 interference (Eyre et al. 2002; Kana and Weiss 2004; Lunstrum and Aoki 2015). Denitrification has similarly been detected on mussels, where it accounted for 5% to 80% of total denitrification rates (Nizzoli et al. 2006). However, given different species and cultivation techniques, these high denitrification rates may not occur on oysters. Oysters cultivated for the half-shell market, like those in this study, are regularly cleaned to prevent epiflora/epifauna growth, which could also potentially impact denitrifying communities. Future research on this topic is needed.

Sediment N accumulation

Sediment accumulation was a more important N sink than denitrification, accounting for an estimated 30% of total N extraction. However, accumulation in sediment is also the most uncertain of the measured pathways because of methodological limitations, as discussed further below. There are currently no data available for N burial in oyster aquaculture sites, but considering estuarine sites in

general, our estimated accumulation rates are comparable to published burial values, which range from 1.3 to 13.7 g N m^{-2} y^{-1} (Boynton et al. 2008; Palinkas and Cornwell 2012). Relative burial rates, i.e., burial (i.e., accumulation) relative to the total particulate N deposition, are also comparable to estuarine averages. Assuming that all deposited N is accounted for in benthic N fluxes (NH_4^+ and N_2) and sediment accumulation, accumulation accounted for 15% and 32% of N deposition at Row and Oyster sites, respectively. Burial has been estimated at 10% of total N sedimentation in the Chesapeake Bay (Boynton et al. 1995), a rate which has been applied in subsequent oyster bioextraction studies (Newell et al. 2005; Carmichael et al. 2012). While the Oyster accumulation rate in our study is relatively high, we expect that this enhancement is spatially limited, as seen by the drastic decrease in NH_4^+ fluxes and sediment N content between the Oyster and Row sites. Nitrogen burial rates in estuaries are known to be higher in areas with high deposition rates such as the Chesapeake Bay and its tributaries (Tappin 2002), so the relatively high accumulation rate measured in the farm may be a reasonable estimate for this site. Burial is highly site-specific however, and likely depends on hydrodynamics and management practices that resuspend sediment and prevent long-term burial. For example, Mallet et al. (2006) found no enhancement in sediment N in an oyster farm that had been cultivated for 20 years, likely due to regular sediment resuspension.

Direct measurement of long-term burial would be difficult at aquaculture sites like the one in this study due to regular farm maintenance. The N accumulation rates presented here are indirect measurements based on differences in sediment N at the farm and Bare sites, and thus represent relative rates in excess of the Bare rates. The absolute rate could be higher or lower, depending on the actual accumulation rate at the Bare site. Along these lines, enhanced accumulation within the farm could result in decreased accumulation in surrounding areas as OM is disproportionately concentrated by oyster feeding activity (Petersen et al. 2012). In this case, the net effect of the farm on basin-scale sediment accumulation may be neutral, or at least more complicated than simple enhancement within

the farm would suggest. It should also be noted that the estimated accumulation may not fully represent long-term burial. The sediment profiles suggest higher N content in the farm even below the 8-cm measurement depth, so long-term burial may be even higher including deeper sediment depths. Conversely, the higher N content in the farm could also represent recently deposited, labile OM that may be remineralized on a longer time scale. Thus, the short-term accumulation of N does not necessarily represent long-term burial. Given these uncertainties, the values presented here should be viewed as indication of a trend of enhanced accumulation, and not as absolute rates. Future studies with long-term, and preferably basin-scale, monitoring would be needed to confirm these results.

Total N removal capacity

The total N extraction capacity of the farm scaled up to the leased area of the inlet accounted for 162% of the estimated TN load, indicating that extractive processes are sufficient to effectively mitigate watershed N loading. Considering only harvest, which has less associated uncertainty than sediment N accumulation and denitrification, 112% of the annual load could still be removed. Cherrystone has a small watershed with low human and livestock population density, so the estimated TN load was small relative to more populated or larger watersheds. However, the TN load relative to estuary size (6,084 kg N km^{-2} estuary y^{-1}) is comparable to other small estuaries in the mid-Atlantic (S Bricker et al. 2008). These results therefore suggest that using oyster aquaculture to mitigate N pollution could be similarly effective in other estuaries, given comparable sub-tidal areas available for aquaculture use.

Previous oyster aquaculture bioextraction studies have found lower removal efficiencies. Carmichael et al. (2012) reviewed existing studies and found estimates of N removal using bivalve aquaculture ranging from 1% to 15% of annual loads, given likely aquaculture densities and space availability. Similar ranges have been found for clam and mussel farms (Bartoli et al. 2001; Cranford et

al. 2007). The higher efficacy in Cherrystone can be attributed both to relatively low TN loading and high space availability for aquaculture. Cherrystone is a shallow water body and one third of its area is already established in shellfish leases. Larger and deeper estuaries may not be able to support such extensive aquaculture use. The extent to which aquaculture can be expanded is a central issue in the debate about oyster aquaculture's efficacy in N extraction. For example, Bricker et al. (2014a) used areal N bioextraction results from the FARM model (57 g N m^{-2}), and estimated that 50% of the Potomac River Estuary TN load could be removed if half of suitable habitat were utilized for aquaculture. A response by Land (2014) contended that this level of bioextraction could not be achieved, with a major point of contention being the number of oysters, and hence area, that can be cultivated. In the case of Cherrystone, bivalve aquaculture area has already been established so spatial planning is not an issue. Although the 2011 NOAA Aquaculture Policy and National Shellfish Initiative (NOAA 2011) promotes expansion of the industry, local regulations and spatial conflicts may prevent expansion to this level in other locations. Thus, the relative efficacy of oyster farms for N extraction will vary by estuary, depending on exploitable space.

N extraction versus N regeneration

The balance between bioextractive pathways and N regeneration pathways like mineralization is another key point of controversy surrounding the efficacy of N bioextraction (Stadmark and Conley 2011). Enhanced NH_4^+ flux is a well-known issue in bivalve aquaculture, with farm rates typically several-fold higher than control sites (Bartoli et al. 2001; Cranford et al. 2007; Stadmark and Conley 2011; Carlsson et al. 2012). In our case, NH_4^+ flux at Oyster sites was at least 17 times higher than Bare sites, and in summer, Oyster rates reached >900 µmol N m^{-2} h^{-1}, which is among the highest rates published for oyster farms. The cumulative NH_4^+ flux for the farm was 140% of the harvested N, and comparable to the total N bioextraction (Figure 5). This may be an overestimate, considering the possibility that the

high rates measured directly under oyster bags (Oyster sites) may be spatially limited. However, even if we use only the Row rates, NH_4^+ mineralization from the farm is still 85% of the harvested N. Scaling up to the total leased area of the inlet, NH_4^+ flux accounts for 158% of the watershed TN load. In other words, while >100% of the TN load can be removed by harvest, an even greater amount of N is regenerated from the sediment. The N cycling rates in excess of the TN load could potentially be supported by marine inputs and recycling of standing stock phytoplankton N, as discussed below. Note that our field study only considered benthic remineralization, and does not consider direct excretion from oysters. If direct excretion of dissolved N were included, the release rate from the farm would be even higher. For example, direct excretion from oysters can contribute 14% to 40% of the total NH_4^+ emitted from oyster reefs (Dame et al. 1992).

Estimated N extraction and regeneration in excess of the TN load could be supported by N sources not contained in the modeled estimate. In addition to terrestrial and atmospheric inputs (both of which are included in the modeled value), reactive N may also be available from tidal import of algae and recycling of in situ N from phytoplankton or sediment (Kemp and Boynton 1984; Carmichael et al. 2012). Previous field measurements and modeling in Cherrystone have shown that tidal import of phytoplankton and/or nutrients contribute significantly to primary productivity (Condon 2005; Kuschner 2015). Internal recycling of in situ N may also be significant. For example, in their study of Cape Cod estuaries, Carmichael et al. (2012) estimated phytoplankton standing stock N at least six times higher than annual terrestrial TN loads. For comparison, we used the same methods to estimate Cherrystone's available N standing stock: multiplying the inlet's average chl *a* concentration of 7.7 $\mu g\ l^{-1}$ (CBP 2012) by an approximate N:chl *a* ratio of 12.8 (MacIntyre et al. 2002) and the mean volume of the inlet, we estimate that 60,713 kg N is available in phytoplankton standing stock, approximately double the annual TN load. Thus, the total N available to oysters, both from recycling and tidal import, is likely sufficient to support the projected N extraction and regeneration rates estimated in this study.

Concern about increased N regeneration from oyster aquaculture is based on the potential negative ecological impacts associated with eutrophication. Oysters do not cause eutrophication directly by adding N to coastal water, but they may exacerbate or concentrate eutrophic conditions by enhancing N cycling. Enhanced N cycling supported by oysters—including increased OM deposition to the sediment, N remineralization, and subsequent support of primary productivity (Pietros and Rice 2003; Murphy et al. 2015)—potentially retains and concentrates N that would otherwise be distributed over larger areas or exported from the coastal system. Thus, even though harvest removes nutrients, if reactive N is disproportionately retained and recycled instead of exported, reactive N may increase in areas around oyster farms. Such an increase in reactive N could potentially lead to negative impacts associated with eutrophication like excessive algal growth and water column anoxia.

However, these consequences of eutrophication depend on site-specific conditions and may not be realized in all locations. In systems with low flushing rates, enhanced N concentrations may support seasonal algae blooms and subsequent decay ("bloom and bust" cycles) that result in water column anoxia (Nizzoli et al. 2007). In systems with high flushing rates like Cherrystone, on the other hand, NH_4^+ and/or secondary primary production may be efficiently exported from the local system, and its fate controlled by conditions downstream. Cherrystone has extremely low ambient NH_4^+ concentrations (typically <1 μM) due to rapid assimilation by primary producers, including macroalgae associated with aquaculture surfaces (Murphy et al. 2015). Farm maintenance at both clam and oyster farms dislodges this algae, and much of it is presumably exported from the system during tidal flushing (Mark Brush, personal communication). Thus, despite enhanced N cycling in the farms, reactive N may not accumulate in the inlet, as it is ultimately exported in particulate form. If maximum, quantifiable removal of N from the aquatic system is desired, aquaculture-supported algae could also be harvested, following the concepts of multi-trophic aquaculture.

In conclusion, while N regeneration rates were high within the farm, and comparable in magnitude to total extractive processes, there is no clear evidence that this regeneration causes negative eutrophic conditions within Cherrystone. High flushing rates may sufficiently distribute regenerated nutrients and associated primary production outside of the inlet. This flushing, combined with the fact that N extraction is significant relative to watershed TN loading indicates that oyster aquaculture can be an effective tool to reduce nutrient concentrations in Cherrystone. Similar efficacy may be expected in water bodies with moderate TN loads, high tidal flushing, and significant area for aquaculture expansion.

Acknowledgements

This research was supported by grants from Virginia Sea Grant's Graduate Student Fellowship program and a student grant from the Virginia Water Resources Research Center. I would like to thank Meigan McManus and Devin Rowell for their assistance with laboratory procedures.

References

Bartoli, M, D Nizzoli, P Viaroli, E Turolla, G Castaldelli, EA Fano, and R Rossi. 2001. Impact of Tapes philippinarum farming on nutrient dynamics and benthic respiration in the Sacca di Goro. *Hydrobiologia* 455: 203–212.

Boesch, DF, RB Brinsfield, and RE Magnien. 2001. Chesapeake Bay Eutrophication. *Journal of Environmental Quality* 30. American Society of Agronomy, Crop Science Society of America, Soil Science Society: 303–320.

Bouwman, L, A Beusen, PM Glibert, C Overbeek, M Pawlowski, J Herrera, S Mulsow, R Yu, and M Zhou. 2013. Mariculture: significant and expanding cause of coastal nutrient enrichment. *Environmental Research Letters* 8: 044026. doi:10.1088/1748-9326/8/4/044026.

Boynton, WR, JH Garber, R Summers, and WM Kemp. 1995. Inputs, transformations, and transport of nitrogen and phosphorus in Chesapeake Bay and selected tributaries. *Estuaries* 18. Springer: 285–314.

Boynton, WR, JD Hagy, JC Cornwell, WM Kemp, SM Greene, MS Owens, JE Baker, and RK Larsen. 2008. Nutrient Budgets and Management Actions in the Patuxent River Estuary, Maryland. *Estuaries and Coasts* 31: 623–651. doi:10.1007/s12237-008-9052-9.

Bricker, S, B Longstaff, W Dennison, A Jones, K Boicourt, C Wicks, and J Woerner. 2008. Effects of nutrient enrichment in the nation's estuaries: a decade of change. *Harmful Algae* 8. Elsevier: 21–32.

Bricker, SB, KC Rice, and OP Bricker III. 2014a. From Headwaters to Coast: Influence of Human Activities on Water Quality of the Potomac River Estuary. *Aquatic Geochemistry* 20: 291–323. doi:10.1007/s10498-014-9226-y.

Bricker, SB, KC Rice, and OP Bricker III. 2014b. Response to L. Land Comment on Bricker, Rice, Bricker (2014) From Headwaters to Coast: Influence of Human Activities on Water Quality of the Potomac River Estuary. Aquatic Geochemistry 20: 291–324. *Aquatic Geochemistry* 20: 459–463. doi:10.1007/s10498-014-9233-z.

Butt, AJ, and BL Brown. 2000. The cost of nutrient reduction: A case study of Chesapeake Bay. *Coastal Management* 28. Taylor & Francis: 175–185.

Carlsson, MS, P Engström, O Lindahl, L Ljungqvist, JK Petersen, L Svanberg, and M Holmer. 2012. Effects of mussel farms on the benthic nitrogen cycle on the Swedish west coast. *Aquaculture Environment Interactions* 2: 177–191. doi:10.3354/aei00039.

Carmichael, RH, W Walton, and H Clark. 2012. Bivalve-enhanced nitrogen removal from coastal estuaries. *Canadian Journal of Fisheries and Aquatic Sciences* 69: 1131–1149. doi:10.1139/F2012-057.

CBP. 2012. Chesapeake Bay Program Data Hub.

Cloern, JE. 2001. Our evolving conceptual model of the coastal eutrophication problem. *Marine ecology progress series* 210: 223–253.

Condon, ED. 2005. Physiological ecology of the cultured hard clam, Mercenaria mercenaria : a case study in Cherrystone Inlet, Virginia. College of William and Mary.

Cornwell, JC, WM Kemp, and TM Kana. 1999. Denitrification in coastal ecosystems: methods, environmental controls, and ecosystem level controls, a review. *Aquatic Ecology* 33: 41–54.

Cranford, P, P Strain, M Dowd, B Hargrave, J Grant, and M Archambault. 2007. Influence of mussel aquaculture on nitrogen dynamics in a nutrient enriched coastal embayment. *Marine Ecology Progress Series* 347: 61–78. doi:10.3354/meps06997.

Dalrymple, DJ, and RH Carmichael. 2015. Effects of age class on N removal capacity of oysters and implications for bioremediation. *Marine Ecology Progress Series* 528: 205–220. doi:10.3354/meps11252.

Dame, RF, JD Spurrier, and RG Zingmark. 1992. In situ metabolism of an oyster reef. *Journal of Experimental Marine Biology and Ecology* 164. Elsevier: 147–159.

Emery, K. 2015. Coastal bivalve aquaculture carbon cycling, spatial distribution and resource use in Virginia, USA and Baja California, Mexico. MSc thesis, University of Virginia, Charlottesville, VA.

Eyre, BD, S Rysgaard, T Dalsgaard, and PB Christensen. 2002. Comparison of Isotope Pairing and N2:Ar Methods for Measuring Sediment Denitrification—Assumptions, Modifications, and Implications. *Estuaries* 25: 1077–1087. doi:10.1007/bf02692205.

Ferreira, JG, A Sequeira, AJS Hawkins, A Newton, TD Nickell, R Pastres, J Forte, A Bodoy, and SB Bricker. 2009. Analysis of coastal and offshore aquaculture: Application of the FARM model to multiple systems and shellfish species. *Aquaculture* 292: 129–138. doi:10.1016/j.aquaculture.2009.03.039.

Grizzle, RE, and K Ward. 2011. *Experimental Quantification of Nutrient Bioextraction Potential of Oysters in Estuarine Waters of New Hampshire. PREP Publications. Paper 18.*

Henriksen, K, and WM Kemp. 1988. Nitrification in estuarine and coastal marine sediments. In *Nitrogen Cycling in Coastal Marine Environments*, ed. TH Blackburn and J. Sorensen, 207–249. John Wiley and Sons, Chichester.

Higgins, CB, K Stephenson, and BL Brown. 2011. Nutrient Bioassimilation Capacity of Aquacultured Oysters: Quantification of an Ecosystem Service. *Journal of Environment Quality* 40: 271. doi:10.2134/jeq2010.0203.

Higgins, CB, C Tobias, MG Piehler, AR Smyth, RF Dame, K Stephenson, and BL Brown. 2013. Effect of aquacultured oyster biodeposition on sediment N2 production in Chesapeake Bay. *Marine Ecology Progress Series* 473: 7–27. doi:10.3354/meps10062.

Kana, TM, JC Cornwell, and L Zhong. 2006. Determination of denitrification in the Chesapeake Bay from measurements of N2 accumulation in bottom water. *Estuaries and coasts* 29. Springer: 222–231.

Kana, TM, and DL Weiss. 2004. Comment on "Comparison of isotope pairing and N2:Ar methods for measuring sediment denitrification" by BD Eyre, S. Rysgaard, T. Dalsgaard, and P. Bondo Christensen. 2002. Estuaries 25: 1077–1087. *Estuaries and Coasts* 27: 173–176.

Kellogg, ML, J Cornwell, M Owens, and K Paynter. 2013. Denitrification and nutrient assimilation on a restored oyster reef. *Marine Ecology Progress Series* 480: 1–19. doi:10.3354/meps10331.

Kellogg, ML, AR Smyth, MW Luckenbach, RH Carmichael, BL Brown, JC Cornwell, MF Piehler, MS Owens, DJ Dalrymple, and CB Higgins. 2014. Use of oysters to mitigate eutrophication in coastal waters. *Estuarine, Coastal and Shelf Science* 151. Elsevier Ltd: 156–168. doi:10.1016/j.ecss.2014.09.025.

Kemp, WM, and WR Boynton. 1984. Spatial and temporal coupling of nutrient inputs to estuarine primary production: the role of particulate transport and decomposition. *Bulletin of Marine Science* 35. University of Miami-Rosenstiel School of Marine and Atmospheric Science: 522–535.

Kemp, WM, WR Boynton, JE Adolf, DF Boesch, WC Boicourt, G Brush, JC Cornwell, et al. 2005. Eutrophication of Chesapeake Bay: historical trends and ecological interactions. *Marine Ecology Progress Series* 303: 1–29. doi:10.3354/meps303001.

Kuschner, MA. 2015. A model of carrying capacity and ecosystem impacts in a large-scale, bivalve dominated agro-ecosystem: hard clam aquaculture in Cherrystone Inlet, VA. Virginia Institute of Marine Science, College of William and Mary.

Land, LS. 2014. Oysters' Impact on Water Quality in the Potomac River Estuary. *Aquatic Geochemistry* 20. Springer: 465–466.

Lunstrum, A, and L Aoki. 2015. Oxygen interference with membrane inlet mass spectrometry may overestimate denitrification rates calculated with the isotope pairing technique. *In preparation*.

MacIntyre, HL, TM Kana, T Anning, and RJ Geider. 2002. Photoacclimation of photosynthesis irradiance response curves and photosynthetic pigments in microalgae and cyanobacteria1. *Journal of phycology* 38. Wiley Online Library: 17–38.

Mallet, AL, CE Carver, and T Landry. 2006. Impact of suspended and off-bottom Eastern oyster culture on the benthic environment in eastern Canada. *Aquaculture* 255: 362–373. doi:10.1016/j.aquaculture.2005.11.054.

Murphy, A, IC Anderson, and M Luckenbach. 2015. Enhanced nutrient regeneration at commercial hard clam (Mercenaria mercenaria) beds and the role of macroalgae. *Marine Ecology Progress Series* 530: 135–151. doi:10.3354/meps11301.

Newell, RIE. 2004. Ecosystem influences of natural and cultivated populations of suspension-feeding bivalve molluscs: a review. *Journal of Shellfish Research* 23: 51–61.

Newell, RIE, TR Fisher, RR Holyoke, and JC Cornwell. 2005. Influence of eastern oysters on nitrogen and phosphorus regeneration in Chesapeake Bay, USA. In *The comparative roles of suspension-feeders in ecosystems*, 47:93–120. Springer.

Newell, RIE, and R Mann. 2012. *Shellfish Aquaculture : Ecosystem Effects , Benthic – Pelagic Coupling and Potential for Nutrient Trading*.

Nixon, SW. 1995. Coastal marine eutrophication: a definition, social causes, and future concerns. *Ophelia* 41. Taylor & Francis: 199–219.

Nizzoli, D, M Bartoli, and P Viaroli. 2007. Oxygen and ammonium dynamics during a farming cycle of the bivalve Tapes philippinarum. *Hydrobiologia* 587: 25–36. doi:10.1007/s10750-007-0683-9.

Nizzoli, D, DT Welsh, EA Fano, and P Viaroli. 2006. Impact of clam and mussel farming on benthic metabolism and nitrogen cycling, with emphasis on nitrate reduction pathways. *Marine Ecology Progress Series* 315: 151–165. doi:10.3354/meps315151.

NOAA. 2011. National Shellfish Initiative.

Palinkas, CM, and JC Cornwell. 2012. A preliminary sediment budget for the Corsica River (MD): improved estimates of nitrogen burial and implications for restoration. *Estuaries and coasts* 35. Springer: 546–558. doi:10.1007/s12237-011-9450-2.

Petersen, JK, B Hasler, K Timmermann, P Nielsen, DB Tørring, MM Larsen, and M Holmer. 2014. Mussels as a tool for mitigation of nutrients in the marine environment. *Marine pollution bulletin* 82. Elsevier Ltd: 137–43. doi:10.1016/j.marpolbul.2014.03.006.

Petersen, JK, K Timmermann, M Carlsson, M Holmer, M Maar, and O Lindahl. 2012. Mussel farming can be used as a mitigation tool--a reply. *Marine pollution bulletin* 64: 452–4; author reply 455–6. doi:10.1016/j.marpolbul.2011.11.027.

Pietros, JM, and MA Rice. 2003. The impacts of aquacultured oysters, Crassostrea virginica (Gmelin, 1791) on water column nitrogen and sedimentation: results of a mesocosm study. *Aquaculture* 220. Elsevier: 407–422.

Rose, J, SB Bricker, M Tedesco, and G Wikfors. 2014. A role for shellfish aquaculture in coastal nitrogen management. *Environmental Science & Technology*. doi:10.1021/es4041336.

Rose, JM, SB Bricker, and JG Ferreira. 2015. Comparative analysis of modeled nitrogen removal by shellfish farms. *Marine Pollution Bulletin* 91. Elsevier Ltd: 185–190. doi:10.1016/j.marpolbul.2014.12.006.

Rose, JM, JG Ferreira, K Stephenson, SB Bricker, M Tedesco, and GH Wikfors. 2012. Comment on Stadmark and Conley (2011) “Mussel farming as a nutrient reduction measure in the Baltic Sea: consideration of nutrient biogeochemical cycles”. *Marine pollution bulletin* 64: 449–51; author reply 455–6. doi:10.1016/j.marpolbul.2011.11.024.

Sebastiano, D, JS Levinton, M Doall, and S Kamath. 2015. Using a Shellfish Harvest Strategy to Extract High Nitrogen Inputs in Urban and Suburban Coastal Bays: Practical and Economic Implications. *Journal of Shellfish Research* 34: 573–583. doi:10.2983/035.034.0242.

Smyth, AR, N Geraldi, and MF Piehler. 2013. Oyster-mediated benthic-pelagic coupling modifies nitrogen pools and processes. *Marine Ecology Progress Series* 493: 23–30. doi:10.3354/meps10516.

STAC. 2013. *Evaluation of the Use of Shellfish as a Method of Nutrient Reduction in the Chesapeake Bay*.

Stadmark, J, and D Conley. 2012. Response to Rose et al. and Petersen et al. *Marine Pollution Bulletin* 64. Elsevier Ltd: 455–456. doi:10.1016/j.marpolbul.2011.12.001.

Stadmark, J, and DJ Conley. 2011. Mussel farming as a nutrient reduction measure in the Baltic Sea: Consideration of nutrient biogeochemical cycles. *Marine Pollution Bulletin* 62. Elsevier Ltd: 1385–1388. doi:10.1016/j.marpolbul.2011.05.001.

Stephenson, K, S Aultman, T Metcalfe, and A Miller. 2010. An evaluation of nutrient nonpoint offset trading in Virginia: A role for agricultural nonpoint sources? *Water Resources Research* 46: W04519. doi:10.1029/2009WR008228.

Tappin, AD. 2002. An examination of the fluxes of nitrogen and phosphorus in temperate and tropical estuaries: current estimates and uncertainties. *Estuarine, Coastal and Shelf Science* 55. Elsevier: 885–901.

Table 1. Oyster measurements

Shell length (mm)	Wet weight (g)	Shell dry weight (g)	Tissue dry weight (g)	Shell %N	Tissue %N	Total N (g)
80.1 ± 0.9	68.1 ± 1.9	46 ± 1.5	2.8 ± 0.1	0.18 ± 0.01	7.16 ± 0.13	0.28 ± 0.01

Mean ± SE, n=20.

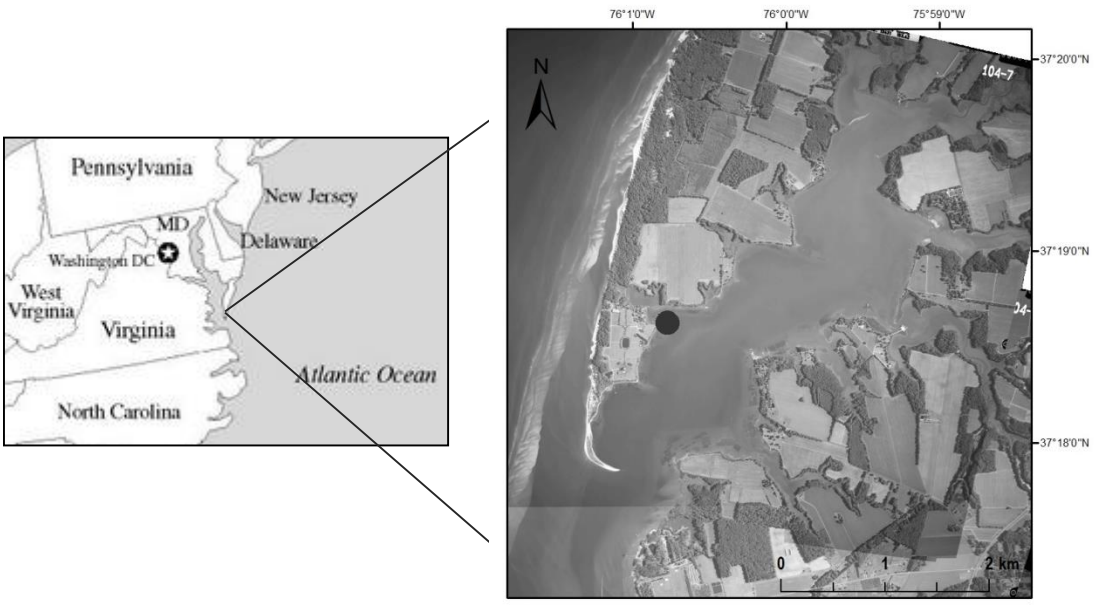

Figure 1. Farm location in Cherrystone Inlet, a tributary of Chesapeake Bay (farm indicated by black circle). Areal photo shows Cherrystone Inlet in the center, and Chesapeake Bay on the left (Virginia Institute of Marine Science, 2012).

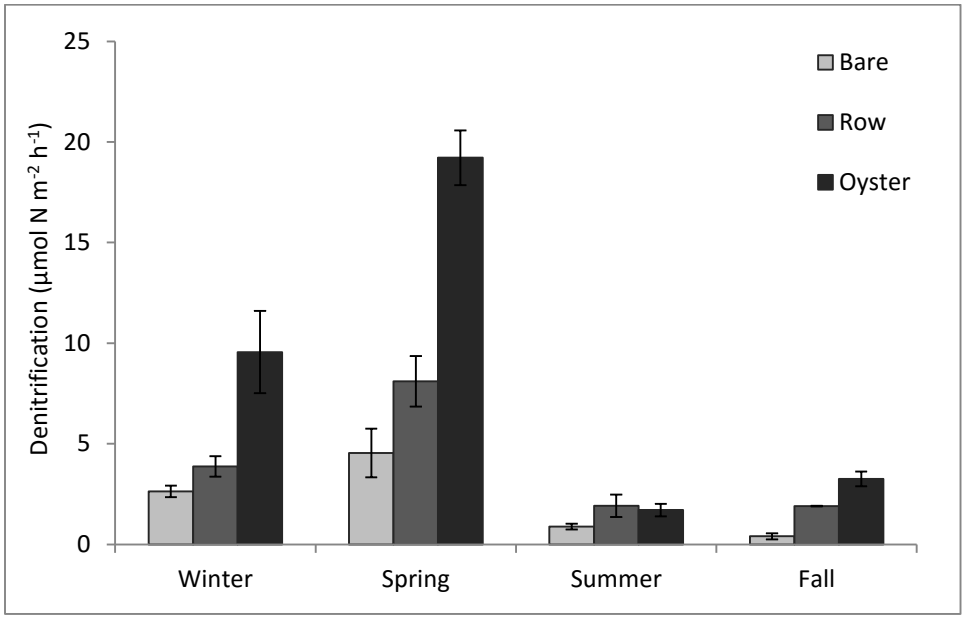

Figure 2. Sediment denitrification rates for the Bare and farm sites (mean ± SE, n=3-8). Figure adapted Chapter 1.

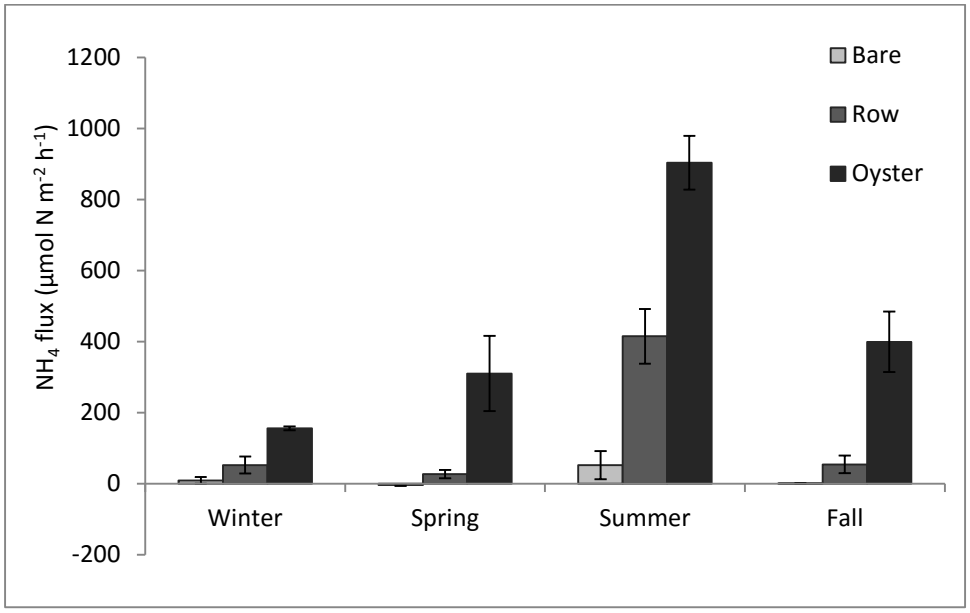

Figure 3. Sediment NH_4^+ flux for the Bare and farm sites (mean ± SE, n=3-8). Figure adapted from Chapter 1.

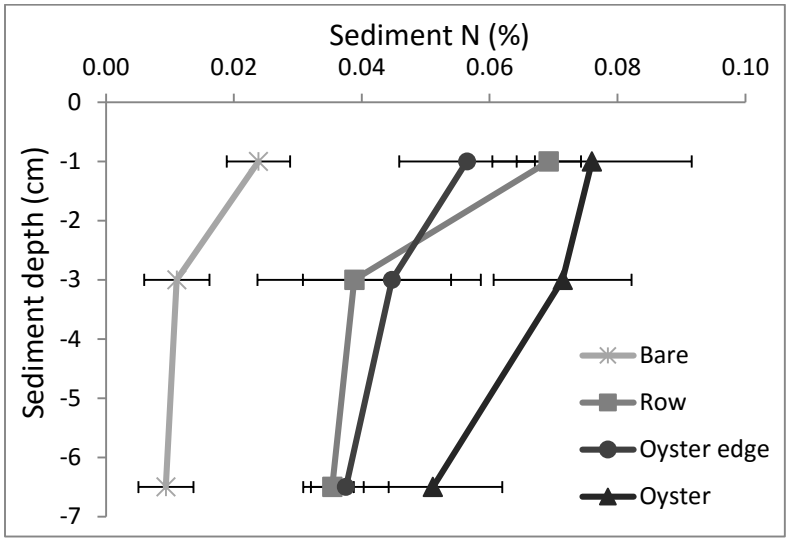

Figure 4. Sediment N content profiles for the Bare and farm sites (mean ± SE, n=6-9)

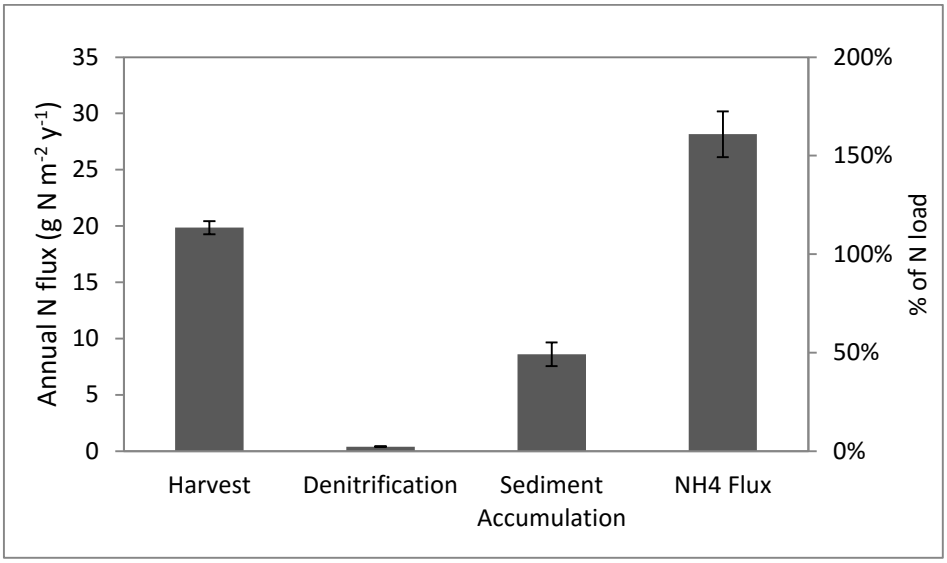

Figure 5. Annual N extraction (harvest, enhanced denitrification and enhanced sediment N accumulation) or regeneration (NH_4^+) measured within the farm for 2013-2014. Enhanced values indicate farm rates in excess of Bare rates. Values are mean ± SE, presented as areal rates (left axis) and % of total N load to Cherrystone Inlet, if extrapolated to all aquaculture leased area (1.9 km^2) (right axis). Harvest is calculated from oyster biomass (n=20); denitrification and NH_4^+ from seasonal flux measurements (n=3-4 per season); and sediment accumulation from core measurements (n=6-9).

Appendix to Chapter 2.

Modeling oyster production and N harvest with the Farm Aquaculture Resource Management (FARM) model*

*This information will be incorporated into Chapter 2 prior to manuscript publication

Introduction

In addition to in situ measurements and actual harvest records, we modeled nitrogen (N) harvest for the study site using the Farm Aquaculture Resource Management (FARM) model (Ferreira et al., 2007). The FARM model has been used in several bioextraction studies (Bricker et al., 2014b; Ferreira et al., 2009; Rose et al., 2015). By including FARM modeled values in our analysis, we hoped to both a) test the accuracy of the model, and b) compare our results to other similar, modeled studies. However, the preliminary model results significantly overestimated N harvest (as described in more detail below), and the source of the overestimate is still not resolved. Thus, I elected not to include the model component in Chapter 2 for the time being. This appendix contains the methods and preliminary results and discussion for the FARM component, which I plan to incorporate into the published manuscript once the issue is resolved.

Methods

The FARM model simulates bivalve production, and biodeposit and nutrient emissions, by integrating physical, biogeochemical, and bivalve growth models. The model requires physical and environmental parameters for the farm site, and cultivation dimensions and practices. We utilized environmental data from various sources collected within Cherrystone Inlet when possible, and from a nearby monitoring station in Chesapeake Bay for variables not measured in the inlet. Current data (maximum currents at spring and neap tides) were collected in Cherrystone during June and July 2014, using a SeaHorse tilt current meter deployed at a near-shore location 500 m from the farm. The six weeks of data were checked for annual representativeness against NOAA current predictions at Cape Charles (station ACT4626). The average maximum spring and neap tides for the measurement period were within 3% of the annual average, so the measured data set was used without adjustment. Tidal range, water depth, and wind speed data were taken from the NOAA Kiptopeke tower for 2014. We

used time series (bimonthly) data collected in Cherrystone Inlet for water quality parameters. These data were collected by the Chesapeake Bay Program (Station C-2) in 2001-2002, and are the most recent time-series water quality data available for Cherrystone (CBP, 2012). We used this data set for temperature, salinity, total suspended solids (TSS), dissolved O_2, dissolved inorganic N (DIN), and turbidity. Particulate organic matter (POM) was calculated based on CBP TSS data, and a POM:TSS ratio of 0.3 calculated from measurements taken near the farm site in 2011-2012 (Murphy, personal communication). Current farm management parameters were used to compare the modeled output to field measurements, including: farm size, seeding density, time to harvest, oyster size at harvest, and observed mortality.

Results and Discussion

The FARM model yielded an estimated annual production of 4,500 kg of oysters (wet weight), which was a very close to our measured value of 4,465 kg. This result is not surprising given the specified seeding density, mortality, and oyster size at harvest. However, net N assimilation was over ten times greater than our N harvest value (221 kg N y^{-1}, compared to 18 kg N y^{-1}). Combining the modeled N value with total production indicates an average oyster N content of 5.0%, which is unrealistically high. The FARM value often yields N assimilation values nearly double measured N harvest, but an overestimated of this magnitude has not been recorded. The model developer is currently investigating this issue (Bricker, personal communication). I will incorporate revised N assimilation values into this discussion, should they become available, prior to publication.

The higher N assimilation rates output by the FARM model compared to field measurements have been explained by distinguishing between assimilation and harvest (Rose et al., 2015). Modeled N assimilation during a single growth cycle includes some oysters that are not harvested during that cycle (e.g., slow-growing individuals still below market size). Based on this fact, it is argued that assimilation

during a given time period is naturally higher than harvest. However, this explanation is insufficient, as the assimilation in the unharvested oysters would then contribute to the following year's harvest. Thus, over the long-term, annual assimilation should equal harvest. If assimilation were in fact higher than harvest, there would be an accumulation of oysters in the farm area, which is clearly not the case. Thus, the existing explanation for FARM model overprediction of N harvest is invalid, and it appears that the model may overestimate N assimilation (and N harvest) in some settings. Bioextraction studies using this model should try to incorporate field measurements in order to verify model results and/or adjust model settings to better align with observations.

References

Bricker, S.B., Rice, K.C., Bricker III, O.P., 2014. From Headwaters to Coast: Influence of Human Activities on Water Quality of the Potomac River Estuary. Aquatic Geochemistry 20, 291–323. doi:10.1007/s10498-014-9226-y

CBP, 2012. Chesapeake Bay Program Data Hub [WWW Document]. URL http://www.chesapeakebay.net/data

Ferreira, J.G., Hawkins, a. J.S., Bricker, S.B., 2007. Management of productivity, environmental effects and profitability of shellfish aquaculture — the Farm Aquaculture Resource Management (FARM) model. Aquaculture 264, 160–174. doi:10.1016/j.aquaculture.2006.12.017

Ferreira, J.G., Sequeira, A., Hawkins, A.J.S., Newton, A., Nickell, T.D., Pastres, R., Forte, J., Bodoy, A., Bricker, S.B., 2009. Analysis of coastal and offshore aquaculture: Application of the FARM model to multiple systems and shellfish species. Aquaculture 292, 129–138. doi:10.1016/j.aquaculture.2009.03.039

Rose, J.M., Bricker, S.B., Ferreira, J.G., 2015. Comparative analysis of modeled nitrogen removal by shellfish farms. Marine Pollution Bulletin 91, 185–190. doi:10.1016/j.marpolbul.2014.12.006